Marine Geology 477 (2024) 107410

Contents lists available at ScienceDirect

Marine Geology

journal homepage: www.elsevier.com/locate/margo

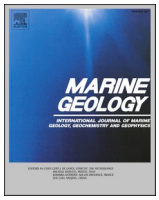

Morphosedimentary evolution of the Belgica Mound Drift: Controls on contourite depositional system development in association with cold-water coral mounds

Alice Ofélia Matossian *, David Van Rooij

Ghent University, Department of Geology, Campus Sterre, Building S8, Krijgslaan 281, 9000 Ghent, Belgium

ARTICLE INFO

Editor: Michele Rebesco

Keywords:
Contourite drift
Bottom current
Cold-water coral mounds
Seismic stratigraphy
Northeast Atlantic
Porcupine Seabight
Quaternary

ABSTRACT

Small-scale contourite drift is an important component of continental margins that can record information about complex oceanographic processes. The Belgica Mound Drift is one example of a small-scale contourite drift. It is formed under the influence of cold-water coral (CWC) mounds and represents one of the most distal contouritic expressions influenced by the Mediterranean Outflow Water (MOW) in the NE Atlantic Ocean. Three distinct evolutionary stages have been identified from new high-resolution pseudo-3D reflection seismic data, each associated with a significant change in paleoceanography, affecting both bottom-current intensity and sediment input. The pre-drift stage (Pliocene–Early Pleistocene) corresponds to the regional RD1 erosive event, which was caused by the reintroduction of the MOW in the Porcupine Seabight, creating a distinct paleotopography that will influence all ensuing sedimentary processes. The second stage (Early Pleistocene–Middle Pleistocene) is the contourite drift inception in two distinct centres of growth, strongly steered by topographic obstacles such as the CWC mounds. During the third and final stage (Middle Pleistocene–present day), the contourite drift is developed under a more stable but less dynamic environment, characterised by more continuous and mounded aggradational stratification. The final stage of the contourite drift is related to the Middle Pleistocene Transition, with a spatially variable reduction in the MOW-related bottom currents and sediment input. The spatial and temporal evolution of this drift shows that its present-day morphology is controlled by the location of initial growth. Evolving moat morphology indicates that the intensity of the bottom currents generally increases during the drift evolution.

This research presents a crucial paradigm for advancing our knowledge of elucidating the complexities of smaller-sized contourite systems in diverse oceanic environments.

1. Introduction

Contourites are deep-sea sedimentary deposits formed under the influence of persistent bottom currents caused by numerous oceanographic processes (Stow et al., 2002; Rebesco, 2005; Rebesco et al., 2014). Their study highlights the past environmental conditions under which the sediment has been deposited and the different factors governing their formation, such as the sediment supply and bottom-current intensity (Mulder et al., 2013; Rebesco et al., 2014). Numerous large-scale contourite drifts, with a size range from 100 to 100,000 km^2, have been identified in the North Atlantic Ocean (Faugères et al., 1993, 1999) and especially on the western side of the Atlantic Ocean (Faugères et al., 1999; Rebesco et al., 2014). These drifts are principally related to the deep thermohaline circulation. Because of their large size and relation with large current systems, those drifts are easily identifiable on bathymetric and regional 2D seismic data and have often been closely observed and examined (Rebesco et al., 2014).

Conversely, smaller-scale drifts (c. 100 km^2; Faugères et al., 1993, 1999) are not always easy to encounter or identify due to their size or because of a poorly known dynamic oceanography. High- to very high-resolution seismic and bathymetric surveys already allowed the observation and identification of such smaller drifts, e.g., in fjord environments (Wils et al., 2021), in the Santaren Channel (Lüdmann et al., 2016), in the Lago Cardiel basin (Gilli et al., 2005), along the Norwegian continental slope (Rebesco et al., 2013), in the South China Sea (Li et al., 2013) and along the Moroccan margin (Vandorpe et al., 2023). Those

* Corresponding author.
E-mail address: alice.matossian@ugent.be (A.O. Matossian).

https://doi.org/10.1016/j.margeo.2024.107410
Received 21 June 2024; Received in revised form 1 October 2024; Accepted 4 October 2024
Available online 13 October 2024

small-scale drifts tend to reflect local processes that are more complex, such as internal waves, tides and bathymetric obstacles that can locally accentuate the bottom currents responsible for the formation of the drift (Rice et al., 1991; De Mol et al., 2002; Van Rooij et al., 2010; Rebesco et al., 2014). Even though large-scale contourite drifts are common and well-known across the world, from abyssal plains to continental margins, there are currently no unambiguous diagnostic criteria for smaller-scale contourite drifts (Rebesco et al., 2014; Van Rooij et al., 2016; Rodrigues et al., 2022). By defining those diagnostic criteria, it may be possible to distinguish small-scale contourite drifts from other deposits, which would consequently help to comprehend the origin and evolution of those drifts. Advances in investigation methods, such as very high-resolution geophysics on smaller-scale contourite drifts and the collection of high-quality data, might allow for fine-tuning their diagnostic potential in the future.

Additionally, there are several examples of small-scale contourite drifts associated with deep-water obstacles, such as cold-water coral (CWC) mounds (Van Rooij et al., 2007; Hanebuth et al., 2015; Hebbeln et al., 2016). Those obstacles (and others) locally modify the path of the bottom currents, intensifying their strength and assisting in local contourite depositional processes. The co-existence of CWC mounds and contourite drifts is widespread along the eastern Atlantic margin, ranging from the Moroccan (Vandorpe et al., 2016) to the Irish margins (Van Rooij et al., 2007), as well as in the Alborán Sea and on the Mexican margin (Hebbeln et al., 2016). Most of those CWC mounds are correlated to intermediate water masses (Henry et al., 2014), such as the Mediterranean Outflow Water (MOW), as they rely on the strong hydrodynamic regime induced by internal waves occurring at the interfaces with other water masses (De Mol et al., 2002; Hernández-Molina et al., 2011; Hebbeln et al., 2016). This, in turn, creates nepheloid layers that facilitate the supply of sediment and food particles (Hebbeln et al., 2016). This could explain why the corals and the contourite drifts are frequently found side-by-side from 200 to 1000 m of water depth, as the distribution of the CWC mounds is more restricted, extending from shallow to intermediate water depths (1000 m) (Viana et al., 2007; Hebbeln et al., 2016).

One of the most notable examples of co-evolution between CWC mounds and contourites, triggered by the presence of the MOW, is

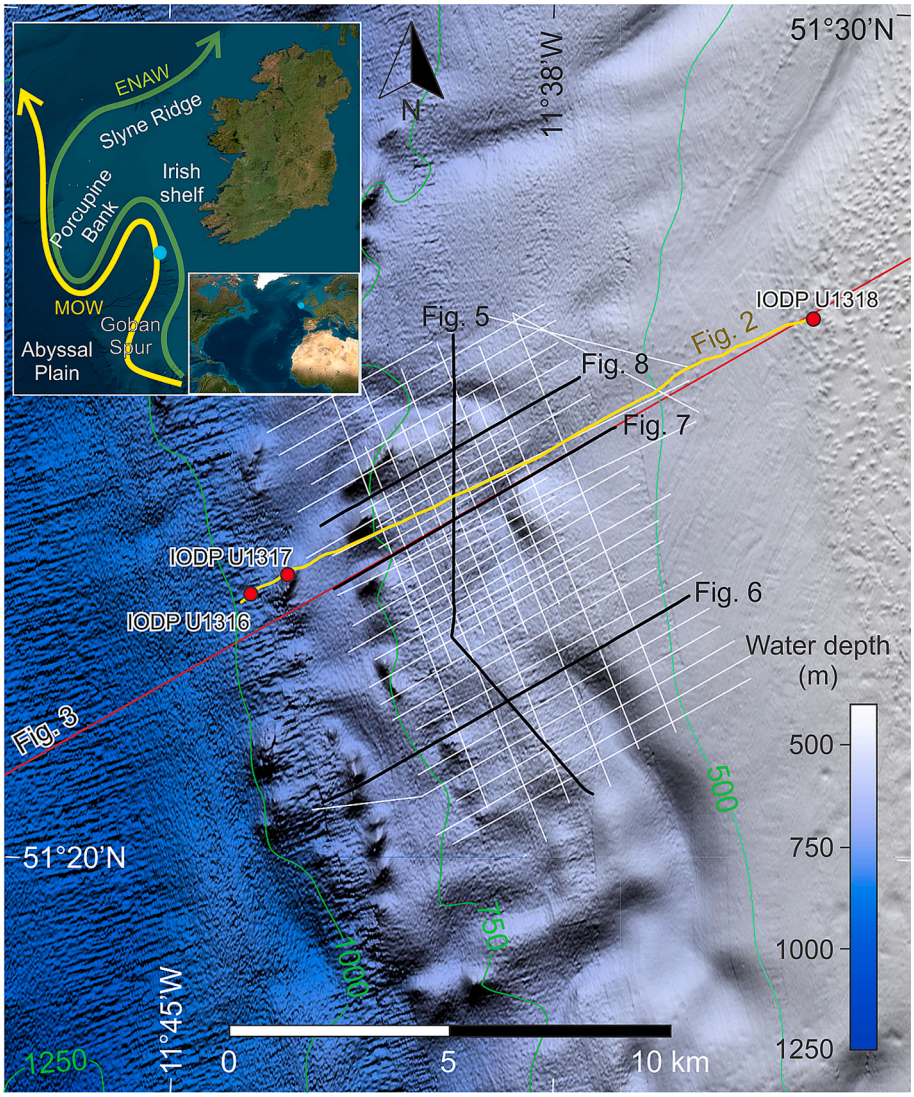

Fig. 1. Bathymetric map of the study area (blue dot in the upper left corner inset) in the Porcupine Seabight, offshore Ireland (adapted from 25 m resolution data from INFOMAR, 2023). The green and yellow arrows represent the intermediate water mass circulation of Eastern North Atlantic Water (ENAW) and Mediterranean Outflow Water (MOW), respectively (upper left corner inset; based on Dullo et al., 2008). The white lines in the main figure represent the seismic lines, whereas the black lines represent the lines shown as figures (Figs. 5–8). The yellow line is seismic line P980521 (Fig. 2). The red line represents the salinity cross-section (Fig. 3). The IODP Exp. 307 coring sites (U1316, U1317 and U1318) are circled in red. (For interpretation of the references to colour in this figure legend, the reader is referred to the web version of this article.)

located in the Porcupine Seabight, offshore Ireland (Hovland et al., 1994; Henriet et al., 1998; De Mol et al., 2002). Those coral communities are composed of *Lophelia pertusa* and *Madrepora oculata* (De Mol et al., 2002), which are deep-sea framework-building corals settling on hard substratum and under vigorous bottom currents (Freiwald et al., 1999; Hebbeln et al., 2016). Based upon the initial seismic stratigraphic studies by Henriet et al. (1998), De Mol et al. (2002), Huvenne et al. (2003) and Van Rooij et al. (2003), the Belgica Mound Province (BMP) and more particularly the Challenger Mound and its surroundings were drilled during IODP Exp. 307 (Ferdelman et al., 2006). The Challenger Mound is located adjacent to a confined contourite drift of around 40 km^2, earlier identified by Van Rooij et al. (2003, 2007) (Fig. 1). The contemporary seismic network was too sparsely spaced to allow any detailed insight into the architecture and evolution of this contourite drift. This necessary insight into its spatial and temporal growth is now made possible by the acquisition of a new densely spaced high-resolution seismic dataset. Due to its particular importance for this paper, we refer to this as the Belgica Mound Drift due to its association with the Belgica CWC mounds.

The initial local seismic stratigraphy, defined by Van Rooij et al. (2003), was ground-truthed during IODP Exp. 307, providing a reliable chronostratigraphy (Kano et al., 2007; Louwye et al., 2008), which was linked to the phases of the CWC mound growth (Huvenne et al., 2009). Nevertheless, the spatial correlation between the actual main body of this drift and the IODP sites was based on sparse seismic data (Fig. 2). IODP site U1318 also did not drill the full record of the contourite drift sequence; only the youngest strata were recovered (Fig. 2). However, the IODP results reported a hiatus of 6 My at site U1318 before the onset of the drift deposition (Kano et al., 2007; Louwye et al., 2008). Since the oldest part of the contourite sequence had not been drilled, the exact onset and extent of this hiatus required re-evaluation. However, at that time, the constraints on the MOW evolution and dynamics were not as well understood as they are now. IODP Exp. 339 in the Gulf of Cadiz (Stow et al., 2013) clearly highlighted the MOW as a key actor in the genesis of several contourite depositional systems (CDS) along the eastern Atlantic continental margin. The work of Hernández-Molina et al. (2006, 2011, 2014) in the Gulf of Cadiz, Hanebuth et al. (2015) at the Galicia Bank, Hernández-Molina et al. (2011) and Collart et al. (2018) at the Ortegal CDS, Ercilla et al. (2008), Van Rooij et al. (2010) and Liu et al. (2020) at the Le Danois CDS and Delivet et al. (2016) at the Goban Spur, respectively presented from a proximal to a distal MOW, delivered new insights into the temporal and lateral variability of this intermediate water mass along the NW European margin and its effects on local bottom-current dynamics. The Cadiz CDS is directly related to the thermohaline circulation and a proximal MOW, whereas in the case of the smaller-scale CDS, located further along the NW European margin, a more distal MOW induces internal waves and tides caused by the interaction with topography, locally enhancing bottom-current intensities.

The investigation of lesser-known small-scale contourite drifts is essential for the future development of diagnostic criteria. Their study is also crucial to consider since it may record local past environmental conditions under which the sediment has been deposited and reworked in various settings, such as continental margins, lakes and fjords. Therefore, this study aims (1) to revise and investigate with greater resolution the previous seismic stratigraphy of the most recent units in the area (Van Rooij et al., 2003, 2009; Huvenne et al., 2009), i.e., the Belgica Mound Drift and the CWC mounds, and to better define the seismic architecture of this confined contourite drift; (2) to refine, in very high-resolution pseudo-3D seismic data, the temporal and spatial variability of this confined contourite drift adjacent to the CWC mounds in order to gain more insight into the contemporary sediment dynamic regime; (3) to correlate the revised and updated Quaternary evolution of the Belgica Mound Drift to the IODP Exp. 307 chronostratigraphy; (4) to evaluate the co-evolution between the Belgica Mound Drift and CWC mounds, starting with the hypothesis of Huvenne et al. (2009) that the mounds were fully grown before the onset of the drift deposition; and (5) to assess the effects of the MOW in one of its most distal contouritic expressions within the eastern Atlantic Ocean.

2. Regional setting

2.1. Geography and geology

The Porcupine Seabight is a large basin (320 × 240 km) with a N—S trend on the western margin of the Irish Shelf, 200 km west of Ireland (Fig. 1). Water depths vary from 350 m in the northern part to 3000 m in the southwest (Naylor and Shannon, 1982). This basin is bounded to the

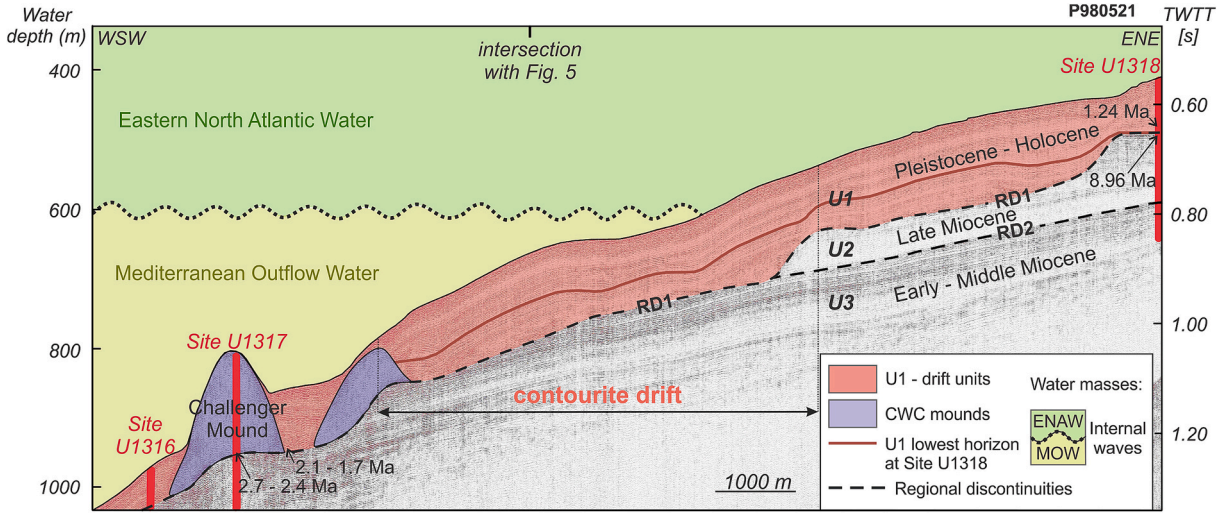

Fig. 2. Seismic profile P980521 (location: Fig. 1) was already studied by Van Rooij et al. (2003, 2007) and used in the framework of IODP Exp. 307 (Ferdelman et al., 2006). The red vertical lines represent the three coring sites defined with the aim of recovering the seismic units previously identified by Van Rooij et al. (2003), including the drift unit U1 in red. The dashed lines are the boundaries (regional discontinuities RD1 and RD2) between seismic units U1, U2 and U3. Their approximative ages are based on Ferdelman et al. (2006). The geological dates around IODP site U1317 (Challenger Mound) are from Huvenne et al. (2009). The ages at IODP site U1318 are from Kano et al. (2007). This profile gives us a better view of the hiatus of missing drift deposits at IODP site U1318 (red horizon in U1). The figure also shows the position of the dynamic interface between Eastern North Atlantic Water (ENAW) and Mediterranean Outflow Water (MOW) in the study area. (For interpretation of the references to colour in this figure legend, the reader is referred to the web version of this article.)

north by the Slyne Ridge and Porcupine Bank, to the east by the Irish Mainland Shelf and to the west by the Porcupine Ridge (Fig. 1). In the southwest, it opens out into the Porcupine Abyssal Plain (4000 m of water depth) (Naylor and Shannon, 1982).

The bathymetry of the Porcupine Seabight shows the complexity of the underlying geology with a Middle to Late Jurassic failed rift and features composed of Precambrian rocks, deformed Upper Paleozoic strata, Mesozoic strata and a Cenozoic sediment cover on top (Naylor and Shannon, 1982). It corresponds to a deep sedimentary trough, i.e., the Porcupine Basin, fault-bounded on its western and eastern margins and filled with post-rift sediments with thicknesses of up to 10 km at their centre (Naylor and Shannon, 1982). The evolution of the basin is directly related to the opening of the North Atlantic Ocean (Johnston et al., 2001) with an episodic crustal extension during the Permo–-Triassic to Early Cretaceous times (Croker and Shannon, 1995; McDonnell and Shannon, 2001), followed by an extensive phase during the Late Jurassic to Early Cretaceous (Johnston et al., 2001; McDonnell and Shannon, 2001). Thermal subsidence occurred afterwards and created an accommodation space for the Late Cretaceous and Cenozoic sediments (McDonnell and Shannon, 2001).

Several margin-wide unconformities have been identified and correlated through stratigraphic and sedimentary comparisons of the Cenozoic evolution of the Porcupine and Rockall basins (McDonnell and Shannon, 2001). Within the Neogene, two major unconformities are relevant for this study. The Early Miocene C20 unconformity was caused by a sea level fall related to the last pulses of the Alpine Orogeny (McDonnell and Shannon, 2001). This unconformity has been identified by Van Rooij et al. (2003) on high-resolution seismic profiles as a regional discontinuity RD2 occurring in the lower Middle Miocene in the BMP (Fig. 2). This regional discontinuity separates seismic stratigraphic units U3 and U2 (Van Rooij et al., 2003). Within unit U3, the local occurrence of upslope migrating sigmoidal deposits already suggests the presence of intensified bottom currents (Van Rooij et al., 2003). Unit U2, characterised by acoustically transparent facies, was deposited over the entire area (Van Rooij et al., 2003) and has a homogenous composition with silty clays of a Late Miocene age (Kano et al., 2007; Louwye et al., 2008).

The Early Pliocene C10 unconformity, observed by Stoker et al. (2001, 2005) along the NW European Atlantic margin, is related to the onset of global cooling and Northern European glaciation. Van Rooij et al. (2003) correlated this to a rather intra-Pliocene regional discontinuity RD1 in the Porcupine Seabight. Several provinces of the CWC coral mounds were also recognised along the northern and eastern slopes of the Porcupine Seabight (De Mol et al., 2002), all rooted upon this RD1 unconformity and associated with relatively strong bottom currents (Van Rooij et al., 2003; Huvenne et al., 2009). Especially in the BMP, along the eastern slope, this has created a typical small-scale contourite depositional system, corresponding to the youngest unit U1 (Van Rooij et al., 2003).

2.2. Hydrographic setting

The present-day water mass stratification related to the Belgica Mound Drift (Figs. 2, 3) shows a seasonal thermocline at a depth of 50 to 70 m (White, 2007). On average, between 0 and 600 m of water depth, the Eastern North Atlantic Water (ENAW), a warm (9.5–12 °C) and saline (35.47–35.6) water mass, can be observed (New et al., 2001; Rice et al., 1991; White, 2007; Dullo et al., 2008). A permanent pycnocline separates the ENAW and the MOW at a depth of approximately 700 m (Pingree and Le Cann, 1990; Rice et al., 1991; White, 2007). A salinity maximum is observed between 800 and 1000 m of water depth and corresponds to the MOW, associated with salinity and temperature ranges of 35.47–35.55 and 8–9.5 °C, respectively (Dullo et al., 2008). The studied seafloor section ranges from 500 to 900 m of water depth and thus correlates to the interface between the ENAW and the MOW (Figs. 2, 3). The main water mass circulation in the present and the past has thus been influenced by the MOW.

The MOW has been active since the end of the Messinian salinity crisis (Khélifi et al., 2009). Since the lower Pliocene, with the start of glacial–interglacial cycles and the onset of the present-day current circulation regime, the MOW has been engaged in the development of contourite drifts and CDSs at intermediate water depths all over the NE Atlantic margin (Khélifi et al., 2009, 2014), from the Gibraltar Strait to the north of the Porcupine Bank (Iorga and Lozier, 1999; van Aken, 2000; McCartney and Mauritzen, 2001). The glacial–interglacial cycles had an impact on the establishment of the modern North Atlantic stratification and the deep-water circulation by changing the production and pathways of water masses, including the MOW (Stow, 1982; Pearson and Jenkins, 1986). The contourite drifts deposited along the NW European margin thus form sedimentary records of the palaeoceanographic evolution of the MOW (Van Rooij et al., 2007; Ercilla et al., 2008; García et al., 2016; Hernández-Molina et al., 2016; Liu et al., 2020). Its reintroduction in the Porcupine Seabight within the course of the Pliocene is thought to be the origin of RD1 (Van Rooij et al., 2003, 2009).

According to White (2001), the general sea surface circulation in the Porcupine Seabight is cyclonic and influenced by two circulation systems: the North Atlantic Current and the Eastern Boundary Current, with at its upper levels the shelf-edge current (SEC), which is a northward-flowing slope current (Pingree and Le Cann, 1989). The SEC carries the upper part of the ENAW northwards along the NE Atlantic margin (New et al., 2001; Rice et al., 1991; White, 2007). The Eastern Boundary Current can be observed near the seafloor, with persistent and along-slope bottom currents that are stronger closer to the seafloor (White, 2001). In addition to this general cyclonic circulation, there are local variations in the direction and speed of those bottom currents on the eastern flank of the Porcupine Seabight and around the depth of the study area (Figs. 2, 3). These variations are caused by a number of processes, including the strong semidiurnal to diurnal tides with a seasonal response (Pingree and Le Cann, 1989, 1990; Rice et al., 1991). The

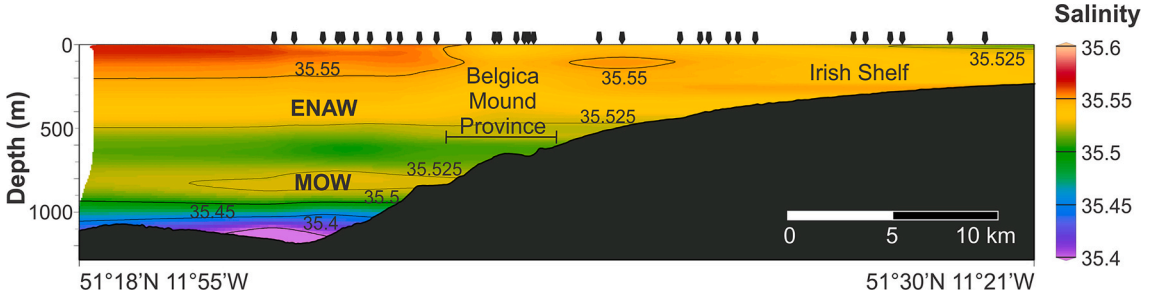

Fig. 3. Salinity-versus-depth cross-section located over the study area (location: Fig. 1), based on CTD data (black arrows) from the World Ocean Database (Boyer et al., 2018). The profile was produced using Ocean Data View (Schlitzer, 2021). ENAW and MOW, respectively, stand for Eastern North Atlantic Water and Mediterranean Outflow Water.

local intensification of the bottom currents is related to internal wave resonance and enhanced diurnal baroclinic tides occurring at the ENAW–MOW pycnocline (Pingree and Le Cann, 1989, 1990; Rice et al., 1991; White, 2007).

3. Materials and methods

The Belgica Mound Drift, 10 km long and 8 km wide (Fig. 1), has been covered by a large network of 1500 km high-resolution single-channel seismic reflection profiles obtained throughout several surveys with RV Belgica from 1997 to 2018 (Van Rooij et al., 2003, 2007). This "legacy" dataset was used to plan a seismic survey with higher-density line spacing covering 50 km^2 located at 460–900 m of water depth over the study area (Fig. 1). This was carried out during the RV Belgica 2019 survey using a SIG sparker source and a single-channel SIG surface streamer. This new dataset yielded 44 high-resolution seismic profiles, from 5 to 10 km in length, spaced between 0.125 and 0.25 nautical miles (nm) in the WSW–ENE direction and between 0.25 and 0.5 nm in the NNW–SSE direction, and is characterised by a vertical resolution of 1.5 m.

During this survey, the seismic source was fired every 2 s at 600 J with a record length of 2.7 s TWT, allowing a penetration depth of around 400 m under the seafloor. During the acquisition, the velocity of the ship was maintained at around 3 knots. The data was digitised with an iXblue Delph system at a sampling frequency of 8 kHz and recorded in SEGY floating-point format. The data was processed in RadExPro 2016.3. Several filters were used on all processed lines: a burst noise removal, a bandpass filter (on average, low-cut ramp of 100 to 150 Hz and high-cut ramp of 1000 to 1500 Hz) and a swell filter. The visualisation and interpretation were carried out using S&P Global Kingdom Geoscience software. The drift and the two major unconformities (RD1 and RD2) had been previously identified by Van Rooij et al. (2003, 2007) and confirmed by IODP Exp. 307 (Ferdelman et al., 2006). The basic concepts of seismic stratigraphy (Mitchum et al., 1977; Badley, 1988) were applied for the identification and description of the spatial and temporal evolution of the drift.

The 25 m resolution-processed bathymetric data (Fig. 1) was made available by INFOMAR (2023) and was used to realise the slope gradient map with Global Mapper software. The combined use of the bathymetry, the slope gradient and the seafloor reflections on the seismic profiles (Fig. 1) assisted in the morphosedimentary mapping. The salinity data (Fig. 3) is based on CTD data from the World Ocean Database (Boyer et al., 2018) and was used for the identification of the water masses. Fig. 3 was produced using Ocean Data View (Schlitzer, 2021).

4. Results

4.1. Morphosedimentary mapping

Although the eastern slope of the Porcupine Seabight has a relatively constant and gentle slope of 1 to 2° towards the west (Fig. 4A), the bathymetry is more variable on a smaller scale in the study area (Fig. 1). Fig. 4B is a revised map of the bathymetric data of a slope-parallel mounded, elongated (separated) and confined contourite drift (Van Rooij et al., 2003), here called the Belgica Mound Drift. It is enclosed by an escarpment, conical CWC mounds (Henriet et al., 1998; De Mol et al., 2002) and moats.

The contourite drift partly overlaps with smaller and steeper CWC mounds along its northern and western edges (Fig. 4B). It is 36 km^2 in size and is located at 600–800 m water depth. This drift is roughly elongated in the NNW–SSE direction and confined in the W–E direction. It is 10 km long and 2.5 to 4 km wide, with the widest part on average in the south of the drift. In more detail, it can be separated into a northern and a southern sector, characterised by a change from a respective N—S and NW–SE orientation halfway along the length of the drift. A crest running is visible alongside the 600 m contour line in the northern sector and at 650 m depth in the southern sector. The slope east of the crest corresponds to the average slope in the area, between 1 and 2° (Fig. 4A), while towards the west, the slope is slightly steeper, up to 7°.

Along its eastern boundary, the southern sector of the drift, as well as its moats, terminate against an escarpment (Fig. 4B). This escarpment has a total length of 8 km (including 3.5 km inside the study area) with a

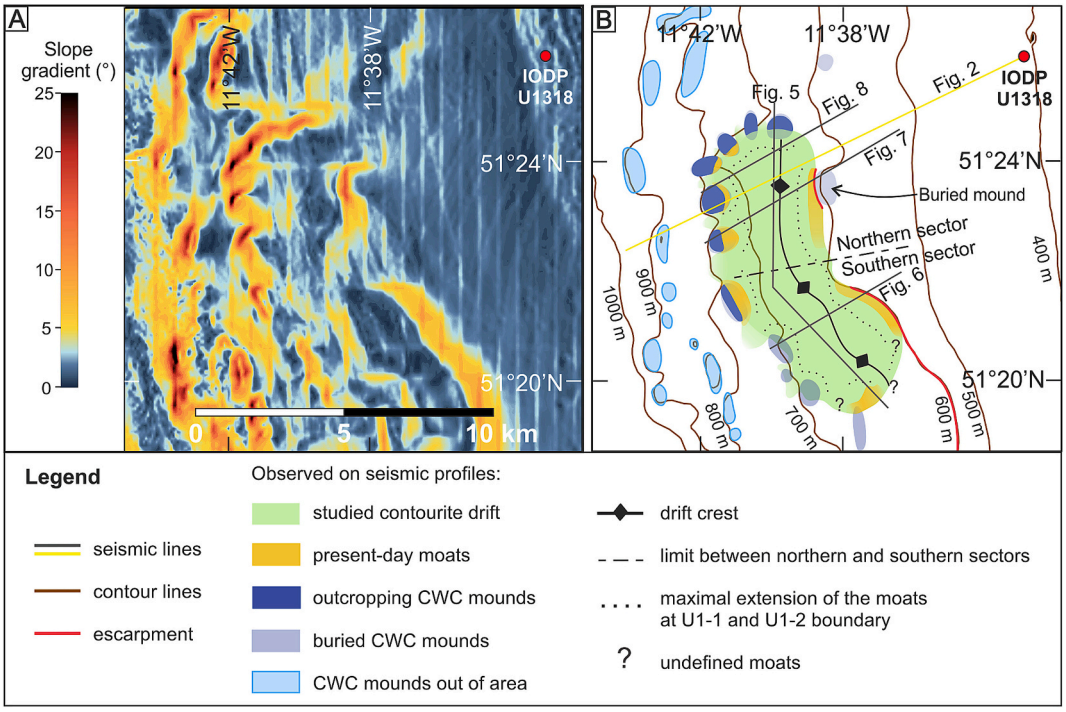

Fig. 4. (A) Slope gradient map and (B) morphosedimentary map of the study area, based on bathymetric data (Fig. 1). The morphosedimentary map represents the present-day surface expression of the drift, including moats and their maximal extension according to the ID1 horizon (Fig. 5).

NW–SE orientation and a slope gradient between 3 and 11° (Fig. 4A), bridging water depths of between 500 and 600 m.

The observed present-day moats (Fig. 4B) have a width between 200 and 650 m in the northern sector and 200 and 500 m in the southern sector. They are typically about 5 m deep, the height difference being measured with respect to the crest of the corresponding horizon of the drift. However, the moat connected to the main escarpment is up to 20 m deep and is significantly longer, up to 6.7 km. The second-longest moat is related to a minor escarpment (3 km long) and is 20 m deep, located at the eastern boundary of the northern sector (Fig. 4B). The smallest moats have a length of about 300 m along the CWC mounds in the northern sector. These moats generally feature an alongslope orientation and are located either upslope of the CWC mounds (W) or downslope of the escarpments (E). However, moats are not observed between the CWC mounds, making it difficult to clearly delimit the boundaries of the drift based on multibeam bathymetry alone, particularly on the NE side of the northern sector. Furthermore, at the transition between the northern and southern sectors, no moat has been observed on the eastern side over a length of 1 km (Fig. 4B). Even along some of the CWC mounds, moats may be absent, such as in the northernmost part of the drift (Figs. 4B, 5). In the southernmost part, only one moat has been observed in the vicinity of buried CWC mounds. The location of the southern moat (Fig. 5) defines the southern limit of the drift.

Twenty-six elongated CWC mounds are spread out over and out of the study area (Fig. 4B). They have an elongated asymmetric elliptic footprint, mostly arranged in a SSE–NNW direction, lined up alongslope on the western edge of the contourite drift, between 600 and 900 m of water depth. More details on the general geometries were described by De Mol et al. (2002). Whereas smaller mounds (typically 10 m high) form single conical structures, larger mounds (at least 500 m wide) are seen to combine into clustered ridge structures. Twelve of those mounds are directly spatially related to the sediment drift as they form the western (Figs. 6–8) and northern (Fig. 5) boundaries of the drift, with inferred slopes from 4 up to 25° (Fig. 4A). The steepest slopes have been observed on the NW side of the mounds. Seven of the mounds (Fig. 4B), especially in the northern sector, are partially outcropping downslope and are buried upslope (Figs. 6–8) along the moats of the drift, while the others are completely buried. The CWC mounds in the northern sector, with a W–E elongation, are more closely spaced (400 to 550 m between mounds), forming a tight barrier at the western side of the sediment drift. The mounds located in the southern sector are more averagely spaced (up to 1100 m between mounds) than in the northern sector and have a N—S elongation.

One isolated feature with a length of 850 m (Fig. 4B), visible on the eastern side of the northern sector of the drift, is completely buried (Fig. 7) and forms on its western side a seemingly small but steep escarpment, characterised by a slope of up to 16° (Fig. 4A) and between 580 and 660 m of water depth.

4.2. Seismic stratigraphy

The erosive event that created RD1 drastically changed the contemporaneous seafloor topography by deeply cutting into older strata (Fig. 5). It had a significant impact on the subsequent depositional and erosive processes and thus on the formation of the contourite drift, corresponding to the youngest unit U1 observed by Van Rooij et al. (2003, 2007). Therefore, the seismic stratigraphic description will be focused on the phases during and after the creation of this RD1 erosive

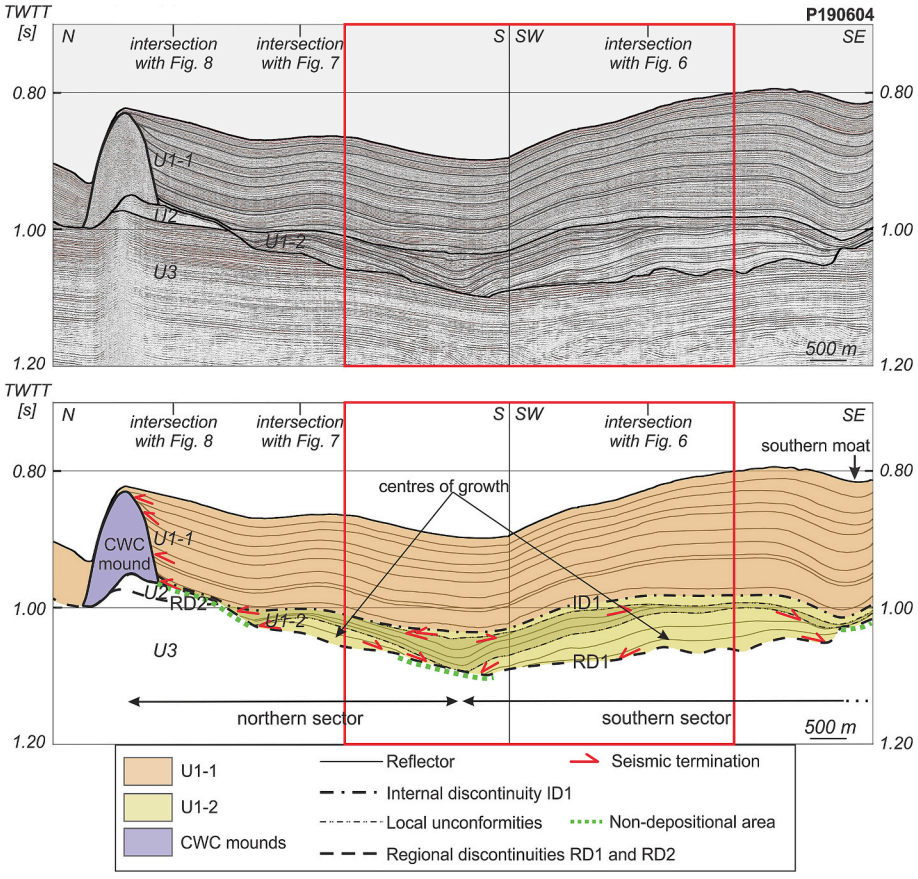

Fig. 5. Seismic profile (location: Fig. 1) along the crest of the drift with the interpreted seismic stratigraphic units. The thick dashed lines represent the regional discontinuities (RD1 and RD2) and the boundary between U1–1 and U1–2 (ID1 horizon; internal discontinuity), while the thinner dashed lines are local unconformities within U1–2. The red rectangle corresponds to a part of the profile used as a reference in Fig. 9. (For interpretation of the references to colour in this figure legend, the reader is referred to the web version of this article.)

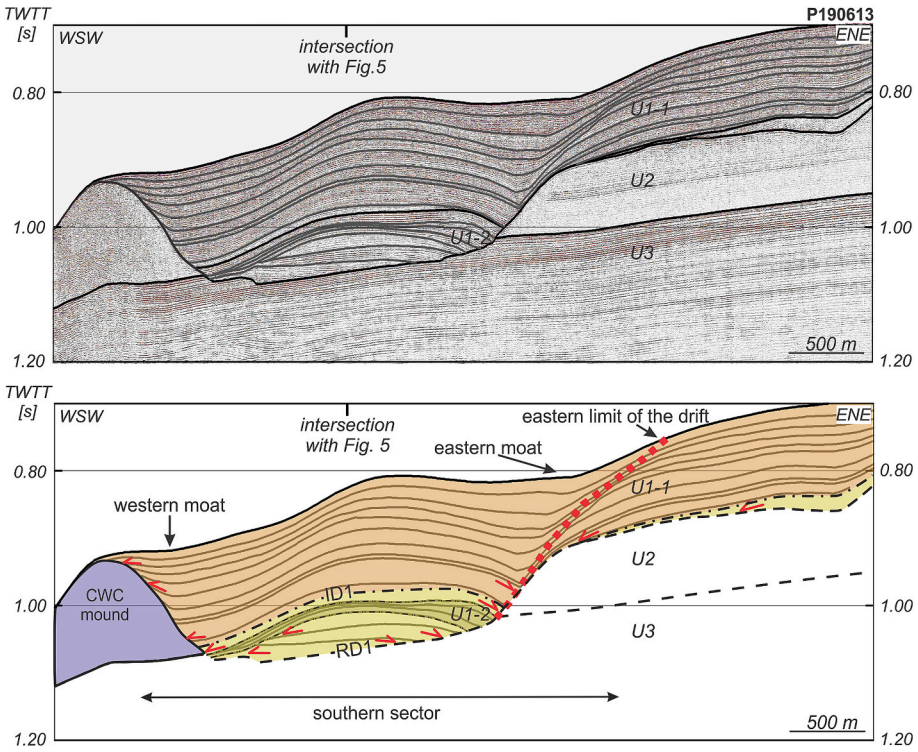

Fig. 6. Seismic profile (location: Fig. 1) across the crest of the southern sector of the drift with the interpreted seismic stratigraphic units. The thick black dashed lines represent the regional unconformities (RD1 and RD2) and the boundary between U1–1 and U1–2 (ID1 horizon; internal discontinuity), while the thinner black dashed lines are local unconformities within U1–2. The red dashed line is the defined eastern limit of the drift. See legend in Fig. 5. (For interpretation of the references to colour in this figure legend, the reader is referred to the web version of this article.)

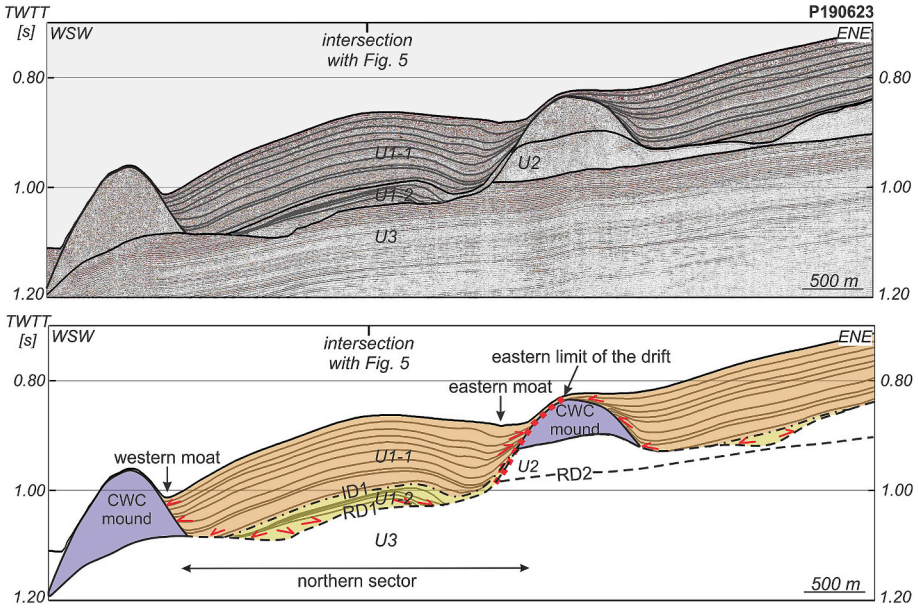

Fig. 7. Seismic profile (location: Fig. 1) across the crest of the northern sector of the drift with the interpreted seismic stratigraphic units. The thick black dashed lines represent the regional unconformities (RD1 and RD2) and the boundary between U1–1 and U1–2 (ID1 horizon; internal discontinuity). The red dashed line is the defined eastern limit of the drift. See legend in Fig. 5. (For interpretation of the references to colour in this figure legend, the reader is referred to the web version of this article.)

discontinuity.

4.2.1. RD1 expression and morphology

The general morphology of the RD1 discontinuity in the study area, in combination with the location of CWC mounds, forms a confined "basin" paleosurface (Fig. 9A, E).

The RD1 discontinuity is an irregular erosive downslope-dipping surface, characterised by deep incisions of up to 200 ms TWT into the underlying units U2 and U3 (Figs. 5–8). Unit U2 is completely absent downslope in the west due to erosion. A few remnants remain at the

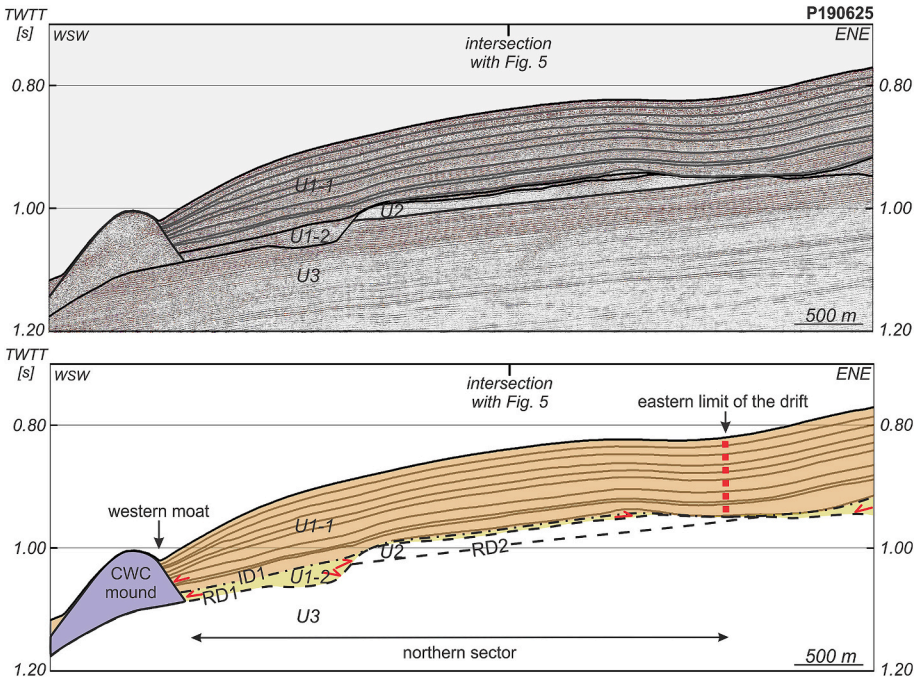

Fig. 8. Seismic profile (location: Fig. 1) across the crest of the northern sector of the drift with the interpreted seismic stratigraphic units. The thick black dashed lines represent the regional discontinuities and the boundary between U1–1 and U1–2 (ID1 horizon; internal discontinuity). The red dashed line is the defined eastern limit of the drift. See legend in Fig. 5. (For interpretation of the references to colour in this figure legend, the reader is referred to the web version of this article.)

northernmost boundary of the study area (Fig. 5), whereas lower U2 remains preserved upslope in the east (Figs. 6–8). Along the eastern boundary of the area, the thickness of U2 decreases from 150 to 0 ms TWT. This has created a N—S escarpment with relatively steep flanks that reach a maximum height of 200 ms TWT and a slope of approximately 15° on the eastern side of the study area (Figs. 6, 9A). The upper part of unit U3 has also been eroded downslope, with predominant erosion in the centre of the area (Fig. 5). Hence, this erosion created at least the eastern flanks of the basin-shaped surface (Fig. 7). The northern and specifically western limits are formed by the alignment of the CWC mounds (Figs. 4, 9A).

These ellipsoidal to conical asymmetric mounds have a broad base up to 1800 m wide and are rooted in alongslope trends on the RD1 unconformity on elevated topographic irregularities (Figs. 5, 7). They are acoustically transparent without any clear internal reflections. Diffraction hyperbolae conceal the true shape of the mounds, especially their base and limits (Figs. 5–8). The size of the mounds decreases from north to south, and their height above RD1 ranges between 35 and 175 ms TWT. Towards the southern part of the area, all mounds are buried under a thin sedimentary cover of up to 20 ms TWT.

The combination of the RD1 paleotopography, including the CWC mounds, is used for the construction of a paleobathymetric map from this composite surface (Fig. 9A). For the objectives of this paper, focusing mainly on the sediment dynamics leading to the deposition of unit U1, it is assumed that the CWC mounds were fully grown before the deposition of unit U1 (Huvenne et al., 2009). This composite paleotopography basically forms a NNW–SSE artificial channel of 2 to 3 km wide and 10 km long, with an average slope between 0 and 3°. Its flanks on the east are about 200 ms TWT high, whereas its slopes range between 13 and 25° at the escarpments and between 6 and 16° in the central area. The western flanks, delimited by CWC mounds, are, on average, 150 ms TWT high with slopes of 20 to 30°. As such, this pre-U1 paleotopography may be considered a peculiar confined basin (or trap) in which unit U1 was deposited.

4.2.2. Post-RD1 deposits

The contourite drift identified by Van Rooij et al. (2003) is formed by unit U1 (Figs. 5–8), covering the entire study area and a part of the CWC mounds. Its seismic facies are characterised by high-frequency, continuous, sub-parallel to mounded reflections with mainly high but variable amplitudes. On a smaller scale, there are various reflection characteristics.

In general, the drift is thinning to the north, with a maximum thickness of up to 250 ms TWT for the southern sector and 200 ms TWT for the northern sector, respectively (Figs. 6, 9E). The maximum thickness is located in the centre of the sectors. The minimum thickness is reached at the extremities of the drift, either in the vicinity of the mounds, near the escarpments, or in the northern part (from 0 to 100–150 ms TWT) (Fig. 9E).

Unit U1 can be subdivided into two sub-units, U1–2 and U1–1, based on a marked difference in reflector configuration (Figs. 5–9). The boundary between both sub-units has been set at the last visible minor internal discontinuity (ID1). In general, the older sub-unit U1–2 is characterised by more chaotic, irregular reflectors and several minor unconformities, whereas sub-unit U1–1 displays continuous, regular and sub-parallel reflectors. Both sub-units have an overall upward convex geometry, flanked by moats. The moats are well developed during the deposition of U1–2 and are progressively phased out within the sediments of U1–1 (Figs. 5–8).

4.2.2.1. Sub-unit 1–2. Sub-unit U1–2 has been deposited directly upon the RD1 erosional unconformity. The reflectors downlap on RD1 in the centre of the deposit (Fig. 5) and on the eastern border (Fig. 6). They also onlap on RD1 and the CWC mounds towards the edges of the drift. Sub-unit U1–2 shows both mounded continuous and irregular reflectors with high lateral variability and several minor unconformities (Fig. 5). The maximum thickness of sub-unit U1–2 is about 80 ms TWT. It is composed of eight different smaller units, each with an average thickness of 16 ms TWT, showing diverse acoustic facies with low, medium and high amplitudes and frequencies (**Table 1 in Supplementary material**). The stacking and stratigraphic relationship between these smaller units allow for the three main growth phases to be distinguished.

The deposition of sub-unit U1–2 was initiated (Figs. 5, 9B) from two

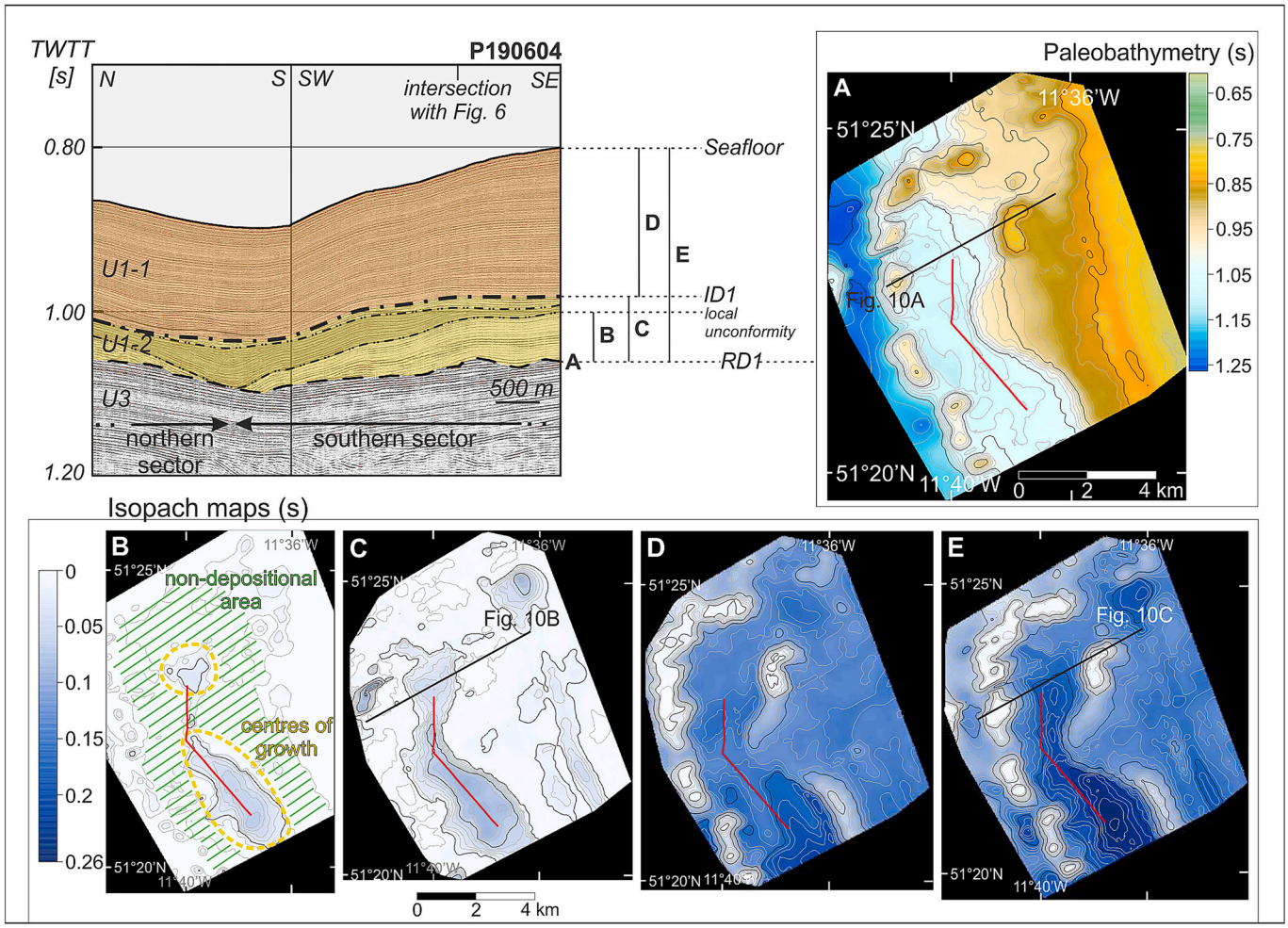

Fig. 9. Section of Fig. 5 (red line in panels A, B, C, D and E), used as a reference to illustrate the drift isopachs and their corresponding reflectors. See legend in Fig. 5. (A) Paleobathymetry map of the RD1 surface (s TWT). The black line corresponds to Fig. 10A. Here, it is assumed that CWC mounds were fully grown before the start of the drift deposition. (B) Isopach map (s TWT) of the sediments deposited between RD1 and a local unconformity. The yellow dashed lines delimit the two centres of growth while the green dashed lines cover the non-depositional area. (C) Isopach map (s TWT) of the sediments deposited between RD1 and ID1 (internal discontinuity), i.e., the complete sub-unit U1–2. The black line corresponds to Fig. 10B. (D) Isopach map (s TWT) of the sediments deposited between ID1 and the seafloor, i.e., the complete sub-unit U1–1. (E) Isopach map (s TWT) of the sediments deposited between RD1 and the seafloor, i.e., the complete unit U1. The black line corresponds to Fig. 10C. (For interpretation of the references to colour in this figure legend, the reader is referred to the web version of this article.)

distinct centres of growth. One centre of growth is located in the northern sector, with a length and width of 2.8 and 1.6 km, respectively, at the end of the first phase. The other centre of growth is located within the southern sector and has a respective length and width of 4.7 km and 2.2 km, displaying a more elongated shape in a NW–SE orientation. This is in contrast to the northern centre, which does not display a clear orientation and has a more circular shape. Both centres are separated from each other by a non-depositional flat area (Fig. 9B). The southern centre of growth is more developed than the northern one, with a thicker sediment deposition of a maximum of 80 ms and 48 ms TWT, respectively. This first phase mainly shows a progradational deposition with a lateral filling of the basin for the northern centre of growth and in a more dominant NW–SE direction for the southern centre of growth.

The second phase is delimited by two minor unconformities (Figs. 5, 9), which can be observed with the entire Belgica Mound Drift. They are irregular in extent, and their style of incision is complex and spatially variable. They cut 1 to 3 ms TWT deep and between 700 and 1000 m wide with the first sub-unit U1–2 deposits at the edges of the drift (Fig. 5). The second phase corresponds to a mixed period with progradational phases along the sides in the W–E direction. At the end of the second phase, the northern and southern centres of growth were 3.2 km long and 2.2 km wide and 4.5 km long and 2.4 km wide, respectively. This was also accompanied by aggradational phases in the middle of the centres of growth towards the N—S and NW–SE direction. The non-depositional area in between the two centres of growth and identified during the first phase has evolved into a concave-up moat. It was progressively filled by 48 ms TWT of sediment (Fig. 5). After that, the two centres of growth were completely connected.

The last phase is mainly progradational (Fig. 9C) in the southern centre of growth (4.7 km long and 2.7 km wide). It corresponds to a thin deposit delimited by two minor unconformities, the top one being the boundary between U1–2 and U1–1 (ID1), which has a conformable character. This deposit is almost absent in the northern centre of the growth, either by a lack of deposition or eroded by the ID1 event. Reflection terminations indicate that ID1 is of erosional origin, and this discontinuity can be mapped throughout the drift.

4.2.2.2. Sub-unit 1–1. Sub-unit U1–1 is a well-stratified unit with mounded continuous regular horizons inherited from the final U1–2 morphology at ID1 (Fig. 5). This unit has continuous seismic characteristics throughout the entire drift and is deposited over the initial two centres of growth (Fig. 9D). In sub-unit U1–1, the two centres of growth correspond to the northern and southern sectors. They are consequently referred to as “sectors” in the next paragraphs. The maximum thickness

of sub-unit U1–1 amounts to 200 ms TWT. The difference in thickness between the two sectors (Fig. 9D) in sub-unit U1–1 is not as straightforward as in sub-unit U1–2 (Fig. 9B, C). Nevertheless, in sub-unit U1–1, the southern sector features higher accumulation rates up to 200 ms TWT, compared to the northern sector, up to 140 ms TWT, which is demonstrated by the isopach maps of sub-unit U1–1 (Fig. 9D) as well as of the entire unit U1 (Fig. 9E). Within sub-unit U1–1, up to 10 smaller cyclic sediment packages with an average thickness of 20 ms TWT can be identified, based on their variable seismic facies, varying between low, medium and high amplitudes and frequencies (**Table 1 in Supplementary material**). At IODP site U1318, only the six top packages are present (Fig. 2). There, and along the edges of the study area, sub-unit U1–1 is directly deposited on top of RD1 and progressively fills the moats. This is in contrast to the centre of the basin, where sub-unit U1–1 directly covers U1–2, separated by ID1. Sub-unit U1–1 shows a downlap configuration on RD1 in the west of the drift (Fig. 7) and in the east (Fig. 6), whereas it shows an onlap on the CWC mounds and RD1 in the west and north (Fig. 7). Still, within the morphology and depositional architecture of sub-unit U1–1, the two sectors of sub-unit U1–2 are reflected. Overall, sub-unit U1–1 displays a progradational depositional pattern near the moats in N—S and W–E directions and is aggradational at the centre of the drifts (Fig. 5).

4.2.2.3. Moats. Conversely to the complex depositional patterns of sub-unit U1–2, the rather uniform nature of the main body of sub-unit U1–1 does not hint at a chaotic depositional pattern indicating vigorous currents. Contrastingly, the evolution of its moats shows a more spatial and temporal variability. In order to better characterise this evolution, the moat classification of Wilckens et al. (2023) is used based on several key seismic profiles (Figs. 5–8).

The maximal extension of the moats at ID1 was between 150 and 1000 m wide. At the onset of sub-unit U1–2, the moats were either exclusively concave-up (western moats in Figs. 6, 8 and southern moat in Fig. 5) or flat-based (eastern moats in Figs. 6, 7). These moats often evolved to a concave-up shape (eastern moat in Fig. 6 and western moat in Fig. 7) during the progressive deposition of the contourite drift. In sub-unit U1–2, the moats mainly mixed depositional–erosional as demonstrated by the downlapping reflectors (both moats in Fig. 6 and western moat in Fig. 7). At the base of sub-unit U1–1, the moats mainly show a concave-up geometry and are either exclusively constructional with onlapping reflectors (southern moat in Fig. 5 and Fig. 6), or they are mixed depositional–erosional moats evolving towards constructional moats (western moat in Fig. 7). During the deposition of sub-unit U1–1, some moats eventually disappear at several locations of the drift (western moat in Fig. 6).

5. Discussion

5.1. Morphosedimentary evolution of the Belgica Mound Drift

The new pseudo-3D seismic stratigraphic analysis of the Belgica Mound Drift architecture suggests that its evolution has followed three main stages (Fig. 10). The conceptual model of the evolution of the drift (Fig. 10) is based on the model developed by Huvenne et al. (2009),

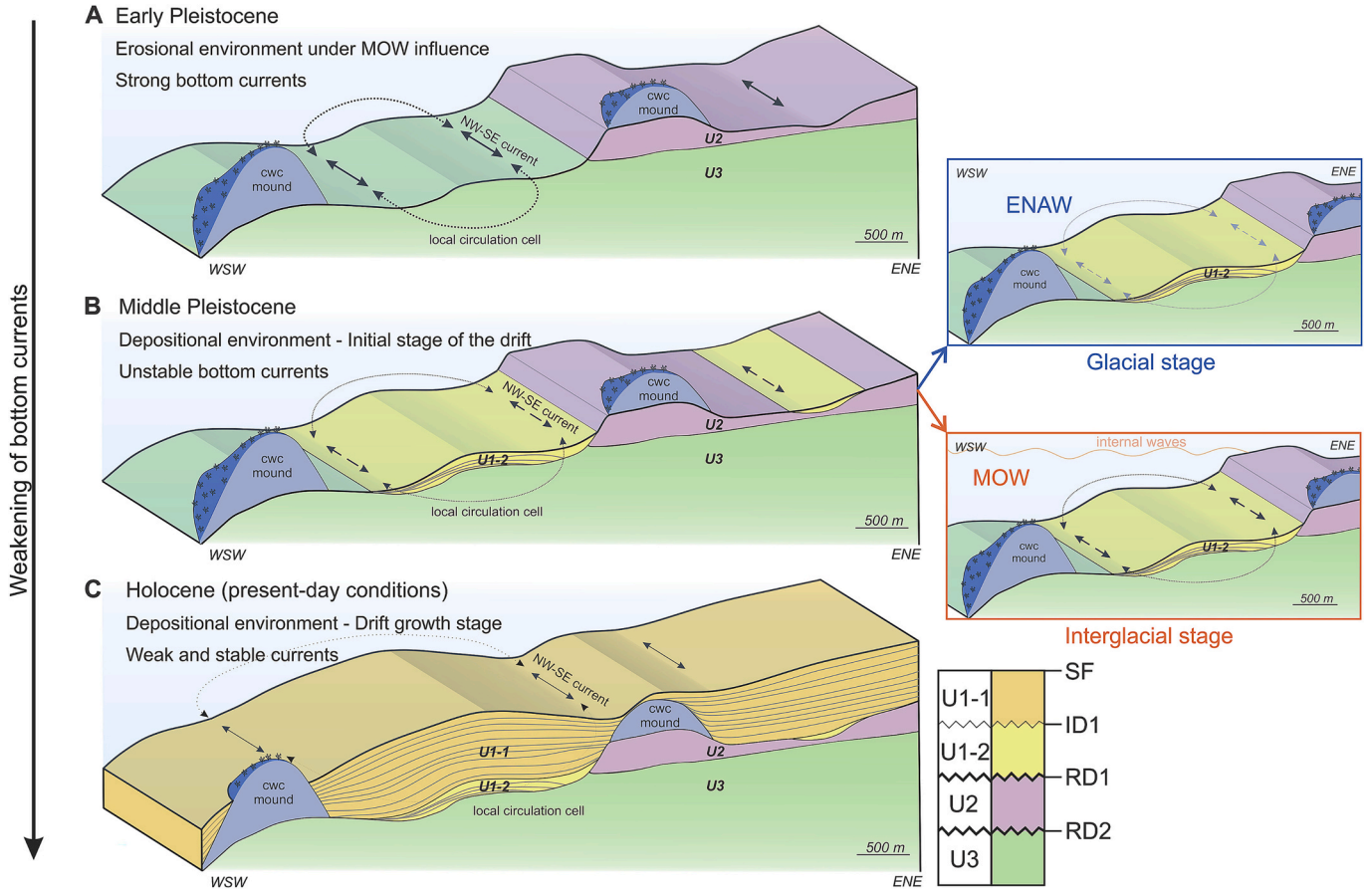

Fig. 10. 3D sketch of the Belgica Mound Drift (northern sector) evolution from the Early Pleistocene to the present day: (A) Before the deposition of the drift (RD1 paleotopography in Fig. 9A); (B) during the onset of the drift (isopach map in Fig. 9C), with an example during the glacial (blue) and interglacial (orange) stages; and (C) during the growth stage of the drift (**isopach** map in Fig. 9E). The arrows correspond to the deduced intensity of the current in the moats, varying from strong (A), strong and unstable (B) to weaker and more stable (C). (For interpretation of the references to colour in this figure legend, the reader is referred to the web version of this article.)

which focused on the CWC mounds. The revised model presented herein focuses on the evolution of the adjacent contourite drift, taking into account the new high-resolution chronostratigraphic framework.

5.1.1. Pre-drift processes related to RD1 (Pliocene–early Pleistocene)

RD1 is a regionally pronounced erosive discontinuity characterised locally by relatively steep escarpments, laying the foundations of the RD1 paleotopography (Figs. 9A, 10A). Its effects can still be observed in present-day bathymetry (Figs. 1, 4). Within the study area, the RD1 unconformity cuts into units U2 and U3 and has almost entirely removed unit U2 (Figs. 5–8). As also observed by Van Rooij et al. (2003) in the channels surrounding the study area, the irregular RD1 topography was likely created by strong and persistent N—S contour currents (Fig. 10A). This peculiar topography contributes to the local intensification of the bottom currents and their consequent erosive nature. Van Rooij et al. (2003) correlated this to the start of the effect of glacial–interglacial cycles on the deep-water circulation as well as to the reintroduction of the MOW in the NE Atlantic during the Pliocene (Stow, 1982; Pearson and Jenkins, 1986). Subsequent research by Khélifi et al. (2014) indicates a reduction in the MOW flow from 2.95 Ma to 2.65 Ma, corresponding to the onset of the major Northern Hemisphere Glaciation. The corresponding sea level falls and subsequent reduction in Atlantic versus Mediterranean exchange, thus influencing the MOW production, may have caused the reduction in the bottom-current intensity in the Porcupine Seabight, bringing the RD1 event to an end. The later reintroduction of the MOW during interglacial periods will have increased the bottom-current intensity again, likely creating hydrodynamic conditions leading to the onset of CWC mound growth (Huvenne et al., 2009; Raddatz et al., 2011), around 2.7 Ma, during the Late Pliocene (Kano et al., 2007).

From seismic profiles alone, it remains complicated to identify the CWC mound growth stages. Hence, it is difficult to compare the evolution of the CWC mounds to the contourite drift evolution. Therefore, it was previously assumed by Huvenne et al. (2009) and Thierens et al. (2010) that the CWC mounds were already fully developed before the deposition of unit U1 (Fig. 10A). The current seismic stratigraphy confirms that the CWC mound growth was initiated before the onset of the contourite drift (Figs. 5–8). As suggested by Van Rooij et al. (2003) and confirmed by the present more detailed dataset, the lower unit U1 horizons show an onlap relation with respect to the CWC mounds (Figs. 5–7), which are asymmetrically embedded in the contourite drift (Figs. 5–8). The CWC mounds thus reached a significant size before the onset of the drift deposition, as evidenced by the basin-like area formed by the CWC mounds' alignment and the steep flanks cut into units U2 and U3 (Fig. 9A). They had a direct influence on the onset of the drift (Fig. 9) and on the evolution of the moats (Fig. 4) since they drove the intensification and pathways of the bottom currents (Van Rooij et al., 2003; Huvenne et al., 2009).

5.1.2. Contourite drift inception (Early Pleistocene–Middle Pleistocene)

The isopach map related to the onset of the contourite drift (Fig. 9B) shows the onset only occurred in the central area of the southern centre of growth, as the oldest sediment package can be observed there (Figs. 5, 9B). This can be interpreted by the action of locally weaker currents on the lee side of the CWC mounds and enhanced currents in the direct vicinity of the CWC mounds, as well as near the steep eastern flanks and in the northern sector. The occurrence of stratigraphically younger contourite drift deposits in the second centre of growth (Fig. 5), located in the central area of the northern sector, indicates the sediment was probably deposited later (Fig. 10B). As such, it is suggested that both centres of growth, both visible in the present-day bathymetry as the two sectors, started growing independently from each other, and were separated by a non-depositional area (Figs. 5, 9B). The difference in shape and elongation between both centres of growth (Fig. 9B) may be related to the inferred circulation pattern of the contemporary bottom currents. The elongated shape of the southern centre of growth (Fig. 9B) is associated with bottom currents with an inferred NW–SE orientation circulating on the western and eastern sides of the drift, represented by the moats. The more circular shape of the northern centre of growth (Fig. 9B) is related to a more complex environment with bottom-current deflection caused by the presence of the CWC mounds, locally accelerating the currents, preventing deposition in the northern centre of growth and between the two centres (Fig. 9B). As such, this may suggest the presence of a local circulation cell, stuck in the northern part of the confined basin, due to topographical deflection (Fig. 9B). The geometry of the moats was exclusively concave-up (western moats in Figs. 6, 8 and southern moat in Fig. 5) or flat-based (eastern moats in Figs. 6, 7) at the start of sub-unit U1–2. However, it evolved towards concave-up (eastern moat in Fig. 6 and western moat in Fig. 7) and mainly a mixed depositional–erosional pattern (both moats in Fig. 6 and western moat in Fig. 7) with the progressive infill of the basin. Also, the seismic stratigraphic analysis of sub-unit U1–2 infers various growing directions and several internal unconformities (Figs. 5–8, 10B). Its rather irregular horizons gradually build up from the central part of the northern and southern centres of growth and progressively join in a later stage of sub-unit U1–2 by the partial filling of the previously non-depositional area (Figs. 5, 9C). This suggests a decrease in the intensity of the local hydrodynamic conditions, leading to less vigorous bottom currents (Fig. 10B). This shows, on average, a slowing down of the NW–SE currents and the circulation cell (Fig. 9C), as well as a likely increase in sediment input in the vicinity of the mounds and flanks where sediment started to accumulate. The internal unconformities, irregular horizons, various growth directions and the mixed nature of the moats highlight unstable currents, occasionally increasing in intensity, inducing possible erosion of sub-unit U1–2, or decreasing in intensity, allowing depositional processes.

5.1.3. Contourite drift development (Middle Pleistocene–present day)

The two centres of growth identified in U1–2 morphologically correspond to the present-day northern and southern sectors (Fig. 9). This inherited morphology results in the continued evolution of the two sectors (Fig. 5), enclosed by the confined basin from CWC mounds and erosive escarpments.

Within sub-unit U1–1, the southern sector still shows a relatively thicker sediment accumulation compared to the northern sector (Fig. 9D). This may still be related to the local intensification of the bottom currents in the northern sector due to the forcing of the currents into a circulation cell by the surrounding CWC mounds. Alternatively, this may indicate proximity to sediment sources from a southern location, such as the Gollum Channels, located south of the study area. Verweirder et al. (2021, 2023) have already demonstrated that this channel system was more active during glacial periods and was the major sediment source in the Porcupine Seabight.

The mapped moats in the southern sector indicate that the bottom currents maintained a NW flow direction throughout U1–1 deposition (Fig. 9D). Within sub-unit U1–1, these moats are mainly concave-up and evolved from mixed depositional–erosional moats towards constructional moats (western moat in Fig. 7). Up to about 25 % of the moats even completely disappear. According to Wilckens et al. (2023), this suggests an average weakening of the bottom currents. Although the intensity of the bottom currents seems to decrease, the moats near the escarpments and CWC mounds are still active (Figs. 4, 6–8). This local intensification would be due to topographic steering where gentle currents are still locally enhanced, as, for example, identified by Vandorpe et al. (2023) offshore Morocco. In contrast with the previous sub-unit, sub-unit U1–1 is characterised by one main growth style (Fig. 5) with continuous and mounded reflectors, prograding along the edges and aggrading along the crests of the two sectors (Figs. 5, 10C). This variation in seismic facies and geometry suggests a switch from an erosive to a depositional-dominated environment with a weakening and possible stabilisation of the bottom currents and a potentially increased sediment input throughout the entire drift (Fig. 10C). This has led to the

progressive disappearing of the moats (Figs. 6–8) and a partial burial of the CWC mounds (Figs. 5–8). This particular switch coincides with the start of deposition at IODP site U1318 (Fig. 2).

5.2. Implications for local chronostratigraphic framework

Sub-unit U1–2 and the oldest strata of U1–1 are deposited within the confined basin created by a combined surface formed by the RD1 paleotopography and CWC mounds. However, the most recent strata of sub-unit U1–1 are also deposited outside this area, such as at IODP site U1318 (Fig. 2), where sub-unit U1–2 is missing (Fig. 2). At IODP site U1318, of the 10 identified sediment packages of sub-unit U1–1 (**Table 1 in Supplementary material**), only the six youngest sediment packages were deposited. Consequently, the oldest contouritic deposits, being the first sediment packages not present on IODP site U1318, are only preserved in the confined drift area. This could be due to a variety of factors, such as stronger bottom currents, likely associated with the SEC, preventing local sedimentation upslope. The observation of four metres of medium to fine sand and gravel lag interbedded with silty clay at the base of U1 at IODP site U1318 (Ferdelman et al., 2006) could corroborate the hypothesis of a long-term non-deposition (Huvenne et al., 2009). The sediment is retained by the nepheloid layer at the boundary between the MOW and ENAW (Figs. 2, 3), as also observed by Hanebuth et al. (2015) along the Galicia margin. This may account for the lack of sediment at IODP site U1318.

Thus, the numerous observations, analyses and dating realised from IODP Exp. 307 only yielded age constraints on the most recent part of the contourite drift (Fig. 2). The onset of unit U1 in the confined basin, and thus of the Belgica Mound Drift, should consequently be older than what has been defined by Kano et al. (2007) at IODP site U1318, i.e., 1.24 Ma, suggesting a probable Early Pleistocene age (Van Rooij et al., 2003, 2007). This may better correspond to the proposed depositional window between 2.1 and 1.7 Ma of sandy contourites at IODP site U1316 at the foot of the Challenger Mound by Huvenne et al. (2009). This window fits with an earlier initiation of the drift, still allowing 0.6 My for the CWC mound to reach a considerable size.

The marked difference in stratigraphic architecture between sub-unit U1–1 and U1–2 was most likely influenced by glacial–interglacial paleoceanographic changes throughout the Pleistocene, influenced by corresponding decreases and rises in sea level (Van Rooij et al., 2009) with a respective absence or presence of the MOW in the Porcupine Seabight (Raddatz et al., 2011). Huvenne et al. (2009), Foubert and Henriet (2009) and Kano et al. (2007) correlated the onset of contourite sedimentation to the first phase of the Middle Pleistocene Transition (MPT). Hence, sub-unit U1–1 would correspond to the units deposited in IODP sites U1316 and U1318 during and following the MPT (1.6–0.5 Ma; Huvenne et al., 2009) (Fig. 2). The MPT was characterised by the initiation of full glacial excentricity-driven conditions with long-term (100 ky) cooling (Lisiecki and Raymo, 2005), increasing of the global ice volume (Berends et al., 2021), leading to decreased bottom-current speeds due to a reduced MOW production and outflow and higher sediment input due to lowered sea levels (Van Rooij et al., 2007; Huvenne et al., 2009). Those conditions during the MPT, while favouring the sedimentation in the area, made the Porcupine Seabight a hydrodynamic less intensive area and reduced the development of CWC mounds (Kano et al., 2007). Whereas decreased bottom currents and higher sediment input are generally advantageous for drift accumulation, this also signifies less favourable conditions for CWC mound growth, leading to CWC decay and potential burial (Hebbeln et al., 2016). After the MPT, a decrease in the MOW influence was also observed in the Goban Spur (Delivet et al., 2016) in contrast with proximal areas such as the Cadiz (Hernández-Molina et al., 2006, 2011, 2014) and the Le Danois CDS (Ercilla et al., 2008; Van Rooij et al., 2010; Liu et al., 2020).

This finally allowed the relatively fast accumulation of sub-unit U1–1 (Fig. 9D), leading to about 200 ms TWT since the MPT. Assuming an average P-wave velocity of 1600 m/s over this unit (Van Rooij et al., 2009), this may roughly have led to an accumulation rate of 17 cm/ky. In their late stage of development, most of the CWC mounds ended up buried under the youngest deposits of sub-unit U1–1, such as the example observed with the isolated eastern CWC mound (Fig. 7). This observation, as well as the moat evolution (Figs. 6–8), indeed highlights a change in the sedimentary environment, evolving from an erosional environment during the initiation of the CWC mounds to a mainly depositional environment in the present day (Fig. 10). Nevertheless, the present-day seabed morphology of the Belgica Mound Drift (Fig. 4) and its moats (Figs. 5–8) testify of the local contemporary (present interglacial) intensification of the bottom currents. The footprint of the RD1 paleotopography on the present-day topography (Figs. 4, 9), as well as the CWC mounds related to internal wave resonance and enhanced diurnal baroclinic tides occurring at the ENAW–MOW pycnocline (Pingree and Le Cann, 1989, 1990; Rice et al., 1991; White, 2007), play a key role in the enhancement of the bottom currents and on the evolution of the contourite drift.

6. Conclusions

This work, focusing on the small-scale Belgica Mound Drift, has shown that a high-resolution pseudo-3D dissection and detailed analysis of a contourite drift yields valuable insights into its spatial and temporal evolution, including its onset and growth patterns. It serves as a showcase of past oceanographic information, specifically for the relative intensity and circulation pattern of the bottom currents at the origin of the drift's morphology.

More specifically, the architecture of this confined contourite drift gave insight into three distinct evolutionary stages, each of which is related to a major change in paleoceanography, affecting both the bottom-current intensity and sediment input. The pseudo-3D dissection allowed for the refinement of the temporal and spatial variability of contourite depositional processes driven by the MOW in its most distal occurrence within the eastern Atlantic Ocean.

- The pre-drift stage (Pliocene–Early Pleistocene) corresponds to the regional RD1 erosive event, which was caused by the reintroduction of the MOW in the Porcupine Seabight, which allowed to shape a peculiar paleotopography, strongly influencing the ensuing sediment dynamics until the present day.
- The second stage (Early Pleistocene–Middle Pleistocene) shows the onset of actual contourite depositional processes, starting from two distinct centres of growth, strongly steered by previously defined topographic obstacles, progressively joining together. The initial deposition happened under the influence of a slightly weakened MOW compared to the first stage. This may be correlated to the general onset of glacial–interglacial cycles at the start of the Quaternary.
- During the third and final stage (Middle Pleistocene–present day), the Belgica Mound Drift development happens under a more stable but less dynamic environment, characterised by more continuous and mounded stratification. This last stage can be fully connected to the effects of the MPT, with a spatial variable reduction in the MOW-related bottom currents, as well as increasing sediment input from potentially nearby sources such as the Gollum Channels. Nevertheless, the present-day bottom currents, in an "interglacial mode", are still strong enough to allow the development of moats due to continued topographic steering (though attenuated with respect to the 2nd phase) by internal wave resonance and tidal enhancement at the MOW–ENAW interface.

During this work, the chronostratigraphic framework, previously established through IODP Exp. 307, required revision since it only provided information regarding the evolution of the most recent stage of the drift. This allowed the onset of contouritic processes to be reset to an earlier date, situated in a window around 2.1 Ma, as defined for IODP

site U1316, but now expanded for the entire Belgica Mound Drift.

Finally, this study also contributed to a better insight into the co-habitation or co-evolution between the contourite drifts and the presence of framework-building ecosystems, such as CWCs. The evolution of the Belgica Mound Drift directly relates to the presence of CWC mounds. Their specific geographic occurrence on an already heavily accentuated paleotopography locally enhanced the intensity and circulation pattern of the bottom currents, especially during the inception of contouritic sedimentation. The combined effects of the RD1 paleotopography and the CWC mounds can still be observed in the present-day bathymetry. This indicates that the mechanisms that shaped the past seabed may still be active today. Therefore, a deeper comprehension of the governing oceanographic processes taking place along the eastern slope of the Porcupine Seabight is required, especially in the drift area.

In general, the complexity of this small-scale contourite deposit is not represented by its youngest part, but it is inherited from its initiation phase. This study is a showcase of the past oceanographic information that is locked in all stages of drift growth. This observation was only possible due to the high-resolution pseudo-3D study of this contourite drift. Hence, it can be argued that valuable paleoceanographic information is only unlocked by choosing an appropriate seismic network (which does not necessarily need to be a costly 3D study), yielding valuable information on both its architectural framework and its spatial and temporal evolution.

Credit authorship contribution statement

Alice Ofélia Matossian: Writing – original draft, Visualization, Investigation, Formal analysis. **David Van Rooij:** Writing – review & editing, Funding acquisition, Data curation, Conceptualization.

Declaration of competing interest

The authors declare that they have no known competing financial interests or personal relationships that could have appeared to influence the work reported in this paper.

Data availability

The seismic reflection data from campaign Belgica 98/01 [doi: https://doi.org/10.1594/PANGAEA.451880] can be found in the PANGAEA data repository. Data from campaign Belgica 2019/17 is part of ongoing research and is not yet available in any repository.

Acknowledgements

This research was conducted in the framework of the FWO project DynaMOD (FWO grant 3G021719). Ship time on RV Belgica was provided by BELSPO and RBINS-OD Nature. We would also like to thank Koen De Rycker, Wim Versteeg and the RV Belgica crews for their help during the acquisition of the seismic data and Thomas Mestdagh for helping with the processing of the dataset. We also would like to thank the editor, Michele Rebesco, Rachel Brackenridge and the anonymous reviewers for their constructive comments, significantly improving this manuscript.

Appendix A. Supplementary data

Supplementary data to this article can be found online at https://doi.org/10.1016/j.margeo.2024.107410.

References

Badley, M.E., 1988. Practical Seismic Interpretation. Prentice Hall.

Berends, C.J., Köhler, R., Lourens, L.J., Wal, R.S.W., 2021. On the cause of the Mid-Pleistocene transition. Rev. Geophys. 59. https://doi.org/10.1029/2020RG000727.

Boyer, T.P., Baranova, O.K., Coleman, C., García, H.E., Grodsky, A., Locarnini, R.A., Mishonov, A.V., Paver, C.R., Reagan, J.R., Seidov, D., Smolyar, I.V., Weathers, K.W., Zweng, M.M., 2018. In: Mishonov, A.V., Techincal Editor (Eds.), World Ocean Database 2018, 87. NOAA Atlas NESDIS.

Collart, T., Verreydt, W., Hernández-Molina, F.J., Llave, E., León, R., Gómez-Ballesteros, M., Pons-Branchu, E., Stewart, H., Van Rooij, D., 2018. Sedimentary processes and cold-water coral mini-mounds at the Ferrol canyon head, NW Iberian margin. Prog. Oceanogr. 169, 48–65. https://doi.org/10.1016/j.pocean.2018.02.027.

Croker, P., Shannon, P., 1995. The petroleum geology of Ireland's offshore basins: Introduction. Geol. Soc. Lond. Spec. Publ. 93, 1–8. https://doi.org/10.1144/GSL.SP.1995.093.01.01.

De Mol, B., Van Rensbergen, P., Pillen, S., Van Herreweghe, K., Van Rooij, D., McDonnell, A., Huvenne, V., Ivanov, M., Swennen, R., Henriet, J.P., 2002. Large deep-water coral banks in the Porcupine Basin, southwest of Ireland. Mar. Geol. 188, 193–231. https://doi.org/10.1016/S0025-3227(02)00281-5.

Delivet, S., Van Eetvelt, B., Monteys, X., Ribó, M., Van Rooij, D., 2016. Seismic geomorphological reconstructions of Plio-Pleistocene bottom current variability at Goban Spur. Mar. Geol. 378, 261–275. https://doi.org/10.1016/j.margeo.2016.01.001.

Dullo, W.-C., Flögel, S., Rüggeberg, A., 2008. Cold-water coral growth in relation to the hydrography of the Celtic and Nordic European continental margin. Mar. Ecol. Prog. Ser. 371, 165–176. https://doi.org/10.3354/meps07623.

Ercilla, G., García-Gil, S., Estrada, F., Gràcia, E., Vizcaino, A., Váquez, J.T., Díaz, S., Vilas, F., Casas, D., Alonso, B., Dañobeitia, J., Farran, M., 2008. High-resolution seismic stratigraphy of the Galicia Bank Region and neighbouring abyssal plains (NW Iberian continental margin). Mar. Geol. 249, 108–127. https://doi.org/10.1016/j.margeo.2007.09.009.

Faugères, J.C., Mézerais, M.L., Stow, D.A.V., 1993. Contourite drift types and their distribution in the North and South Atlantic Ocean basins. Sediment. Geol. 82, 189–203. https://doi.org/10.1016/0037-0738(93)90121-K.

Faugères, J.-C., Stow, D.A.V., Imbert, P., Viana, A., 1999. Seismic features diagnostic of contourite drifts. Mar. Geol. 162, 1–38. https://doi.org/10.1016/S0025-3227(99)00068-7.

Proceedings of the IODP, 307. In: Ferdelman, T.G., Kano, A., Williams, T., Henriet, J.-P., Expedition 307 Scientists (Eds.), 2006. Proceedings of the IODP. Integrated Ocean Drilling Program. https://doi.org/10.2204/iodp.proc.307.2006.

Foubert, A., Henriet, J.-P., 2009. Nature and significance of the recent Carbonate Mound Record: The Mound Challenger Code. Springer Berlin, Heidelberg. https://doi.org/10.1007/978-3-642-00290-8.

Freiwald, A., Wilson, J., Henrich, R., 1999. Grounding Pleistocene iceberg shape recent deep-water coral reefs. Sediment. Geol. 125, 1–8. https://doi.org/10.1016/S0037-0738(98)00142-0.

García, M., Hernández-Molina, F.J., Alonso, B., Vázquez, J.T., Ercilla, G., Llave, E., Casas, D., 2016. Erosive sub-circular depressions on the Guadalquivir Bank (Gulf of Cadiz): Interaction between bottom current, mass-wasting and tectonic processes. Mar. Geol. 378, 5–19.

Gilli, A., Anselmetti, F.S., Ariztegui, D., Beres, M., McKenzie, J.A., Markgraf, V., 2005. Seismic stratigraphy, buried beach ridges and contourite drifts: the late Quaternary history of the closed Lago Cardiel basin, Argentina (49°S). Sedimentology 52, 1–23. https://doi.org/10.1111/j.1365-3091.2004.00677.x.

Hanebuth, T.J.J., Zhang, W., Hofmann, A.L., Löwemark, L.A., Schwenk, T., 2015. Oceanic density fronts steering bottom-current induced sedimentation deduced from a 50 ka contourite-drift record and numerical modeling (off NW Spain). Quat. Sci. Rev. 112, 207–225. https://doi.org/10.1016/j.quascirev.2015.01.027.

Hebbeln, D., Van Rooij, D., Wienberg, C., 2016. Good neighbours shaped by vigorous currents: Cold-water coral mounds and contourites in the North Atlantic. Mar. Geol. 378, 171–185. https://doi.org/10.1016/j.margeo.2016.01.014.

Henriet, J.P., De Mol, B., Pillen, S., Vanneste, M., Van Rooij, D., Versteeg, W., Croker, P. F., Shannon, P.M., Unnithan, V., Bouriak, S., Chachkine, P., Belgica 97 Shipboard Party, 1998. Gas hydrate crystals may help build reefs. Nature 391, 648–649. https://doi.org/10.1038/35530.

Henry, L.-A., Frank, N., Hebbeln, D., Wienberg, C., Robinson, L., de Flierdt, T., van Dahl, M., Douarin, M., Morrison, C.L., Correa, M.L., Rogers, A.D., Ruckelshausen, M., Roberts, J.M., 2014. Global Ocean conveyor lowers extinction risk in the deep sea. Deep. Res. I Oceanogr. Res. Pap. 88, 8–16. https://doi.org/10.1016/j.dsr.2014.03.004.

Hernández-Molina, F.J., Llave, E., Stow, D.A.V., García, M., Somoza, L., Vázquez, J.T., Lobo, F.J., Maestro, A., Díaz del Río, V., León, R., Medialdea, T., Gardner, J., 2006. The contourite depositional system of the Gulf of Cádiz: a sedimentary model related to the bottom current activity of the Mediterranean outflow water and its interaction with the continental margin. Deep Sea Res. Part II Top. Stud. Oceanogr. 53, 1420–1463. https://doi.org/10.1016/j.dsr2.2006.04.016.

Hernández-Molina, F.J., Serra, N., Stow, D.A.V., Llave, E., Ercilla, G., Van Rooij, D., 2011. Along-slope oceanographic processes and sedimentary products around the Iberian margin. Geo-Mar. Lett. 31, 315–341. https://doi.org/10.1007/s00367-011-0242-2.

Hernández-Molina, F.J., Stow, D.A.V., Alvarez-Zarikian, C.A., Acton, G., Bahr, A., Balestra, B., Ducassou, E., Flood, R., Flores, J.-A., Furota, S., Grunert, P., Hodell, D., Jimenez-Espejo, F., Kim, J.K., Krissek, L., Kuroda, J., Li, B., Llave, E., Lofi, J., Lourens, L., Miller, M., Nanayama, F., Nishida, N., Richter, C., Roque, C., Pereira, H., Sanchez Goñi, M.F., Sierro, F.J., Singh, A.D., Sloss, C., Takashimizu, Y., Tzanova, A., Voelker, A., Williams, T., Xuan, C., 2014. Onset of Mediterranean outflow into the North Atlantic. Science 344, 1244–1250. https://doi.org/10.1126/science.1251306.

Hernández-Molina, F.J., Sierro, F.J., Llave, E., Roque, C., Stow, D.A.V., Williams, T., Lofi, J., Van der Schee, M., Arnáiz, A., Ledesma, S., Rosales, C., Rodríguez-Tovar, F.

J., Pardo-Igúzquiza, E., Brackenridge, R.E., 2016. Evolution of the gulf of Cadiz margin and Southwest Portugal contourite depositional system: Tectonic, sedimentary and paleoceanographic implications from IODP expedition 339. Mar. Geol. 377, 7–39. https://doi.org/10.1016/j.margeo.2015.09.013.

Hovland, M., Croker, P.F., Martin, M., 1994. Fault-associated seabed mounds (carbonate knolls?) off western Ireland and north-West Australia. Mar. Pet. Geol. 11, 232–246. https://doi.org/10.1016/0264-8172(94)90099-X.

Huvenne, V.A.I., De Mol, B., Henriet, J.-P., 2003. A 3D seismic study of the morphology and spatial distribution of buried coral banks in the Porcupine Basin, SW of Ireland. Mar. Geol. 198, 5–25. https://doi.org/10.1016/S0025-3227(03)00092-6.

Huvenne, V.A.I., Van Rooij, D., De Mol, B., Thierens, M., O'Donnell, R., Foubert, A., 2009. Sediment dynamics and palaeo-environmental context at key stages in the Challenger cold-water coral mound formation: Clues from sediment deposits at the mound base. Deep. Res. I Oceanogr. Res. Pap. 56, 2263–2280. https://doi.org/10.1016/j.dsr.2009.08.003.

INFOMAR, 2023. INFOMAR Marine Data Download Portal [WWW Document].

Iorga, M.C., Lozier, M.S., 1999. Signatures of the Mediterranean outflow from a North Atlantic climatology: 2. Diagnostic velocity fields. J. Geophys. Res. Oceans 104, 26011–26029. https://doi.org/10.1029/1999JC900204.

Johnston, S., Dore, A., Spencer, A., 2001. The Mesozoic evolution of the Southern North Atlantic region and its relationship to basin development in the South Porcupine Basin, offshore Ireland. Geol. Soc. London Spec. Publ. 188, 237–263. https://doi.org/10.1144/GSL.SP.2001.188.01.14.

Kano, A., Ferdelman, T.G., Williams, T., Henriet, J.-P., Ishikawa, T., Kawagoe, N., Takashima, C., Kakizaki, Y., Abe, K., Sakai, S., Browning, E.L., Li, X., Integrated Ocean Drilling Program Expedition 307 Scientists, 2007. Age constraints on the origin and growth history of a deep-water coral mound in the Northeast Atlantic drilled during Integrated Ocean Drilling Program Expedition 307. Geology 35, 1051–1054. https://doi.org/10.1130/G23917A.1.

Khélifi, N., Sarnthein, M., Andersen, N., Blanz, T., Frank, M., Garbe-Schonberg, D., Haley, B.A., Stumpf, R., Weinelt, M., 2009. A major and long-term Pliocene intensification of the Mediterranean outflow, 3.5-3.3 Ma ago. Geology 37, 811–814. https://doi.org/10.1130/G30058A.1.

Khélifi, N., Sarnthein, M., Frank, M., Andersen, N., Garbe-Schönberg, D., 2014. Late Pliocene variations of the Mediterranean outflow. Mar. Geol. 357, 182–194. https://doi.org/10.1016/j.margeo.2014.07.006.

Li, H., Wang, Y., Zhu, W., Xu, Q., He, Y., Tang, W., Zhuo, H., Wang, D., Wu, J., Li, D., 2013. Seismic characteristics and processes of the Plio-Quaternary unidirectionally migrating channels and contourites in the northern slope of the South China Sea. Mar. Pet. Geol. 43, 370–380. https://doi.org/10.1016/j.marpetgeo.2012.12.010.

Lisiecki, L.E., Raymo, M.E., 2005. A Pliocene-Pleistocene stack of 57 globally distributed benthic delta O-18 records. Paleoceanography 20, PA1003. https://doi.org/10.1029/2004PA001071.

Liu, S., Hernández-Molina, F.J., Ercilla, G., Van Rooij, D., 2020. Sedimentary evolution of the Le Danois contourite drift systems (southern Bay of Biscay, NE Atlantic): a reconstruction of the Atlantic Mediterranean Water circulation since the Pliocene. Mar. Geol. 427, 106217. https://doi.org/10.1016/j.margeo.2020.106217.

Louwye, S., Foubert, A., Mertens, K., Van Rooij, D., The IODP Expedition 307 Scientific Party, 2008. Integrated stratigraphy and palaeoecology of the lower and Middle Miocene of the Porcupine Basin. Geol. Mag. 145, 321–344. https://doi.org/10.1017/S0016756807004244.

Lüdmann, T., Paulat, M., Betzler, C., Möbius, J., Lindhorst, S., Wunsch, M., Eberli, G.P., 2016. Carbonate mounds in the Santaren Channel, Bahamas: a current-dominated periplatform depositional regime. Mar. Geol. 376, 69–85. https://doi.org/10.1016/j.margeo.2016.03.013.

McCartney, M., Mauritzen, C., 2001. On the origin of the warm inflow to the Nordic Seas. Prog. Oceanogr. 51, 125–214. https://doi.org/10.1016/S0079-6611(01)00084-2.

McDonnell, A., Shannon, P.M., 2001. Comparative Tertiary stratigraphic evolution of the Porcupine and Rockall basins. Geol. Soc. London Spec. Publ. 188, 323–344. https://doi.org/10.1144/GSL.SP.2001.188.01.19.

Mitchum, R.M.J., Vail, P.R., Sangree, J.B., 1977. Stratigraphic Interpretation of Seismic Reflection patterns in Depositional Sequences. In: Payton, C.E. (Ed.), Seismic Stratigraphy: Applications to Hydrocarbon Exploration, the American Association of Petroleum Geologist, Tulsa, 26, pp. 117–133.

Mulder, T., Hassan, R., Ducassou, E., Zaragosi, S., Gonthier, E., Hanquiez, V., Marchès, E., Toucanne, S., 2013. Contourites in the Gulf of Cadiz: a cautionary note on potentially ambiguous indicators of bottom current velocity. Geo-Mar. Lett. 33, 357–367. https://doi.org/10.1007/s00367-013-0332-4.

Naylor, D., Shannon, P.M. (Eds.), 1982. Geology of Offshore Ireland and West Britain, Softcover Reprint of the Original 1st ed, 1982 edition. Springer, London.

New, A.L., Barnard, S., Herrmann, P., Molines, J.-M., 2001. On the origin and pathway of the saline inflow to the Nordic Seas: insights from models. Prog. Oceanogr. 48, 255–287. https://doi.org/10.1016/S0079-6611(01)00007-6.

Pearson, I., Jenkins, D.G., 1986. Unconformities in the Cenozoic of the North-East Atlantic. In: Summerhayes, C.P., Shackleton, N.J. (Eds.), North Atlantic Palaeoceanography. Soc. London Spec. Publ, Geol, pp. 79–86.

Pingree, R.D., Le Cann, B., 1989. Celtic and Armorican slope and shelf residual currents. Prog. Oceanogr. 23, 303–338. https://doi.org/10.1016/0079-6611(89)90003-7.

Pingree, R.D., Le Cann, B., 1990. Structure, strength and seasonality of the slope currents in the Bay of Biscay region. J. Mar. Biol. Assoc. U. K. 70, 857–885. https://doi.org/10.1017/S0025315400059117.

Raddatz, J., Rüggeberg, A., Margreth, S., Dullo, W.-C., 2011. Paleoenvironmental reconstruction of Challenger Mound initiation in the Porcupine Seabight, NE Atlantic. Mar. Geol. 282, 79–90. https://doi.org/10.1016/j.margeo.2010.10.019.

Rebesco, M., 2005. Sedimentary Environments: Contourites. In: Selley, R.C., Cocks, L.R. M., Plimer, I.R. (Eds.), Encyclopedia of Geology. Elsevier, Oxford, pp. 513–527. https://doi.org/10.1016/B0-12-369396-9/00497-4.

Rebesco, M., Wåhlin, A., Laberg, J.S., Schauer, U., Beszczynska-Möller, A., Lucchi, R.G., Noormets, R., Accettella, D., Zarayskaya, Y., Diviacco, P., 2013. Quaternary contourite drifts of the Western Spitsbergen margin. Deep-Sea Res., Part 1 Oceanogr. Res. Pap. 79, 156–168. https://doi.org/10.1016/j.dsr.2013.05.013.

Rebesco, M., Hernández-Molina, F.J., Van Rooij, D., Wåhlin, A., 2014. Contourites and associated sediments controlled by deep-water circulation processes: State-of-the-art and future considerations. Mar. Geol. 352, 111–154. https://doi.org/10.1016/j.margeo.2014.03.011.

Rice, A.L., Billett, D.S.M., Thurston, M.H., Lampitt, R.S., 1991. The institute of oceanographic sciences biology programme in the Porcupine Seabight: background and general introduction. J. Mar. Biol. Assoc. U. K. 71, 281–310. https://doi.org/10.1017/S0025315400051614.

Rodrigues, S., Hernández-Molina, F.J., Fonnesu, M., Miramontes, E., Rebesco, M., Campbell, D.C., 2022. A new classification system for mixed (turbidite-contourite) depositional systems: examples, conceptual models and diagnostic criteria for modern and ancient records. Earth Sci. Rev. 230, 104030. https://doi.org/10.1016/j.earscirev.2022.104030.

Schlitzer, R., 2021. Ocean Data View [WWW Document].

Stoker, M.S., Van Weering, T.C.E., Svaerdborg, T., 2001. A Mid- to late Cenozoic tectonostratigraphic framework for the Rockall Trough. Geol. Soc. London Spec. Publ. 188, 411–438. https://doi.org/10.1144/GSL.SP.2001.188.01.26.

Stoker, M.S., Praeg, D., Hjelstuen, B.O., Laberg, J.S., Nielsen, T., Shannon, P.M., 2005. Neogene stratigraphy and the sedimentary and oceanographic development of the NW European Atlantic margin. Mar. Pet. Geol. 22, 977–1005. https://doi.org/10.1016/j.marpetgeo.2004.11.007.

Stow, D.A.V., 1982. Bottom currents and contourites in the North Atlantic. Bull. Inst. Géol. Bassin Aquitaine 31, 151–166.

Stow, D.A.V., Faugères, J.-C., Howe, J.A., Pudsey, C.J., Viana, A.R., 2002. Bottom currents, contourites and deep-sea sediment drifts: current state-of-the-art. Geol. Soc. Lond. Mem. 22, 7–20. https://doi.org/10.1144/GSL.MEM.2002.022.01.02.

Stow, D.A.V., Hernández-Molina, F.J., Llave, E., Bruno, M., García, M., Díaz del Rio, V., Somoza, L., Brackenridge, R.E., 2013. The Cadiz Contourite Channel: Sandy contourites, bedforms and dynamic current interaction. Mar. Geol. 343, 99–114. https://doi.org/10.1016/j.margeo.2013.06.013.

Thierens, M., Titschack, J., Dorschel, B., Huvenne, V.A.I., Wheeler, A.J., Stuut, J.B., O'Donnell, R., 2010. The 2.6 Ma depositional sequence from the Challenger cold-water coral carbonate mound (IODP Exp. 307): sediment contributors and hydrodynamic palaeo-environments. Mar. Geol. 271, 260–277. https://doi.org/10.1016/j.margeo.2010.02.021.

van Aken, H.M., 2000. The hydrography of the mid-latitude Northeast Atlantic Ocean: II: the intermediate water masses. Deep. Res. I Oceanogr. Res. Pap. 47, 789–824. https://doi.org/10.1016/S0967-0637(99)00112-0.

Van Rooij, D., De Mol, B., Huvenne, V., Ivanov, M., Henriet, J.-P., 2003. Seismic evidence of current-controlled sedimentation in the Belgica mound province, upper Porcupine slope, southwest of Ireland. Mar. Geol. 195, 31–53. https://doi.org/10.1016/S0025-3227(02)00681-3.

Van Rooij, D., Blamart, D., Kozachenko, M., Henriet, J.-P., 2007. Small mounded contourite drifts associated with deep-water coral banks, Porcupine Seabight, NE Atlantic Ocean. Geol. Soc. Lond. Spec. Publ. 276, 225–244. https://doi.org/10.1144/GSL.SP.2007.276.01.11.

Van Rooij, D., Huvenne, V.A.I., Blamart, D., Henriet, J.-P., Wheeler, A., de Haas, H., 2009. The Enya mounds: a lost mound-drift competition. Int. J. Earth Sci. 98, 849–863. https://doi.org/10.1007/s00531-007-0293-9.

Van Rooij, D., Iglesias, J., Hernández-Molina, F.J., Ercilla, G., Gomez-Ballesteros, M., Casas, D., Llave, E., De Hauwere, A., Garcia-Gil, S., Acosta, J., Henriet, J.-P., 2010. The Le Danois Contourite Depositional System: Interactions between the Mediterranean Outflow Water and the upper Cantabrian slope (North Iberian margin). Mar. Geol. 274, 1–20. https://doi.org/10.1016/j.margeo.2010.03.001.

Van Rooij, D., Campbell, C., Rueggeberg, A., Wahlin, A., 2016. The contourite log-book: significance for palaeoceanography, ecosystems and slope instability. Mar. Geol. 378, 1–4. https://doi.org/10.1016/j.margeo.2016.05.018.

Vandorpe, T., Martins, I., Vitorino, J., Hebbeln, D., García, M., Van Rooij, D., 2016. Bottom currents and their influence on the sedimentation pattern in the El Arraiche mud volcano province, southern Gulf of Cadiz. Mar. Geol. 378, 114–126.

Vandorpe, T., Delivet, S., Blamart, D., Wienberg, C., Bassinot, F., Mienis, F., Stuut, J.-B. W., Van Rooij, D., 2023. Palaeoceanographic and hydrodynamic variability for the last 47 kyr in the southern Gulf of Cádiz (Atlantic Moroccan margin): Sedimentary and climatic implications. Depositional Rec. 9, 30–51. https://doi.org/10.1002/dep2.212.

Verweirder, L., Van Rooij, D., White, M., Van Landeghem, K., Bossée, K., Georgiopoulou, A., 2021. Combined control of bottom and turbidity currents on the origin and evolution of channel systems, examples from the Porcupine Seabight. Mar. Geol. 442, 106639. https://doi.org/10.1016/j.margeo.2021.106639.

Verweirder, L., Van Rooij, D., Georgiopoulou, A., 2023. Margin processes sculpting a land-detached canyon-channel system: the Gollum Channel System in the Porcupine Seabight. Front. Earth Sci. 11. https://doi.org/10.3389/feart.2023.1285171.

Viana, A.R., Almeida, W., Nunes, M.C.V., Bulhões, E.M., 2007. The economic importance of contourites. Geol. Soc. Lond. Spec. Publ. 276, 1–23. https://doi.org/10.1144/GSL.SP.2007.276.01.01.

White, M., 2001. Hydrography and Physical Dynamics at the NE Atlantic Margin that Influence the Deep Water Cold Coral Reef Ecosystem. EU ACES-ECOMOUND Internal Report. Department of Oceanography, NUI, Galway.

White, M., 2007. Benthic dynamics at the carbonate mound regions of the Porcupine Sea Bight continental margin. Int. J. Earth Sci. 96, 1–9. https://doi.org/10.1007/s00531-006-0099-1.

Wilckens, H., Schwenk, T., Lüdmann, T., Betzler, C., Zhang, W., Chen, J., Hernández-Molina, F.J., Lefebvre, A., Cattaneo, A., Spieß, V., Miramontes, E., 2023. Factors controlling the morphology and internal sediment architecture of moats and their associated contourite drifts. Sedimentology 70, 1472–1495. https://doi.org/10.1111/sed.13093.

Wils, K., Wermersche, M., Van Rooij, D., Lastras, G., Lamy, F., Arz, H.W., Siani, G., Bertrand, S., Van Daele, M., 2021. Late Holocene current patterns in the northern Patagonian fjords recorded by sediment drifts in Aysén Fjord. Mar. Geol. 441, 106604. https://doi.org/10.1016/j.margeo.2021.106604.